Controlling Carbodiimide-Driven Reaction Networks Through Reversible Formation of Pyridine Adducts

Supporting Information

William S. Salvia, Georgia Mantel, Nirob K. Saha, Chamoni W. H. Rajawasam, Dominik Konkolewicz, C. Scott Hartley**

Department of Chemistry & Biochemistry, Miami University, Oxford, OH 45056, United States
scott.hartley@miamioh.edu

Table of Contents

1. Materials

Unless otherwise noted, all starting materials, reagents, and solvents were purchased from commercial sources and used without purification. Chromatographic separations were performed using flash chromatography on silica gel 60 (particle size 43-60 mm). All chromatography conditions have been reported as column height × diameter in centimeters. Reaction progress was monitored by thin-layer chromatography (TLC) on glass-backed silica gel plates. TLC plates were visualized using a handheld UV lamp (254 nm). ^{1}H and ^{13}C NMR spectra were recorded at 400 or 500 MHz, calibrated using residual undeuterated solvent as an internal reference ($CHCl_3$, δ 7.27 and 77.2 ppm), reported in parts per million relative to trimethylsilane (TMS, δ 0.00 ppm), and presented as follows: chemical shift (δ ppm), multiplicity (s = singlet, br s = broad singlet, d = doublet, dd = doublet of doublets, ddd = doublet of doublet of doublets, t = triplet, m = multiplet), coupling constants (*J*, Hz).

Scheme S1: Synthesis of **Ac** (avg. n = 11-12)

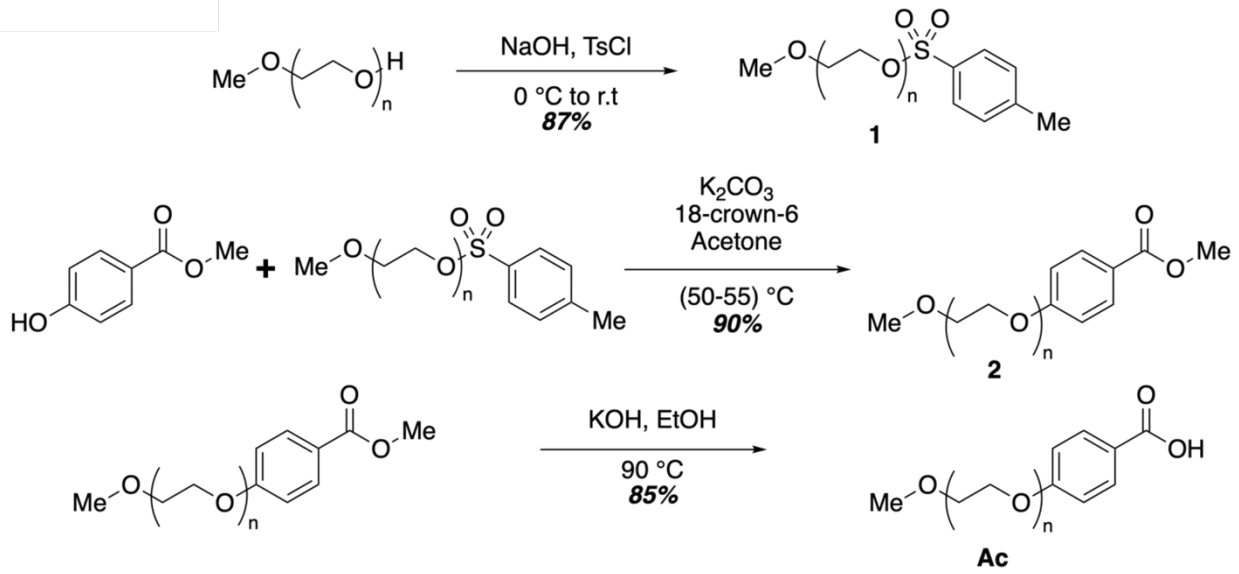

Tosylated PEG-550

A solution of NaOH (5.6 g, 140 mmol) in water (30 mL) and *p*-toluenesulfonyl chloride (11.5 g, 60.3 mmol) in THF (20 mL) was added dropwise to a stirred solution of average molecular weight 550 poly(ethylene glycol) (PEG-550, 30.0 g, 54.6 mmol, avg. n = 11-12) in 4:1 THF:H_2O (250 mL) at 0 °C over 20 min. The reaction was slowly warmed to room temperature. After 40 h, the reaction mixture was diluted by the addition of H_2O (100 mL) and Et_2O (100 mL). The layers were separated, and the aqueous layer was extracted with Et_2O (3 × 100 mL). The combined organic extracts were dried over $MgSO_4$, filtered, and concentrated under reduced pressure to give compound **1** as a colorless oil (33.3 g, 87%). ^{1}H NMR (400 MHz, $CDCl_3$) δ 7.81 – 7.77 (m, 2H), 7.35 – 7.32 (m, 2H), 4.16 – 4.13 (m, 2H), 3.68 – 3.52 (m, 47H), 3.37 (s, 3H), 2.44 (s, 3H). ^{13}C NMR (101 MHz, $CDCl_3$) δ 144.99, 133.16, 130.02, 128.17, 72.11, 70.92, 70.88, 70.78, 70.74, 70.69, 69.44, 68.85, 59.23, 21.84.

Ester 2

Compound **1** (7.9 g, 11.2 mmol) was added to a stirred solution of methyl 4-hydroxybenzoate (1.5 g, 10.1 mmol), K_2CO_3 (7.1 g, 51.8 mmol), and 18-crown-6 (0.34 g, 1.4 mmol) in acetone (75 mL). The reaction mixture was heated at 50–55 °C for 40 h, at which point it was cooled to room temperature and water (200 mL) was added. The resulting mixture was extracted with ethyl acetate (3 × 100 mL). The combined organic extracts were dried over $MgSO_4$, filtered, and concentrated under reduced pressure. The residue was purified via flash chromatography (15 × 5.0 cm, dichloromethane to 1:20 methanol/dichloromethane) to afford **2** as a white solid (6.4 g, 90%). ^{1}H NMR (400 MHz, $CDCl_3$) ^{1}H NMR (400 MHz, $CDCl_3$) δ 7.99-7.96 (m, 2H), 6.94-6.92 (m, 2H), 4.18 (dd, *J* = 5.4, 4.1 Hz, 2H), 3.89 – 3.86 (m, 4H), 3.74 – 3.71 (m, 2H), 3.69 – 3.58 (m, 44H), 3.38 (s, 3H). ^{13}C NMR (101 MHz, $CDCl_3$) δ 167.05, 162.77, 131.77, 130.05, 128.22, 122.92, 114.40, 72.16, 71.11, 70.86, 70.84, 70.80, 70.75, 69.77, 67.78, 59.28, 52.09.

Compound Ac

KOH (2.1 g, 37.4 mmol) was added to a stirred solution of **2** (6.2 g, 8.8 mmol) in ethanol (100 mL). The reaction mixture was heated to 90 °C for 24 h, cooled to room temperature, poured into water (100 mL), and acidified with 1 M HCl(aq) to pH 3. The resulting mixture was extracted with dichloromethane (3 × 50 mL). The combined organic layers were extracted by saturated $NaHCO_3$(aq) solution (3 × 100 mL). The combined aqueous layers were acidified to pH 3 by the slow addition of 1 M HCl and again extracted with dichloromethane (3 × 50 mL). The combined organic extracts were dried over $MgSO_4$, filtered, and concentrated under reduced pressure to give compound **Ac** (5.0 g, 85%) as a white solid. ^{1}H NMR (400 MHz, $CDCl_3$) δ 8.03 – 8.00 (m, 2H), 6.96-6.92 (m, 2H), 4.19 (dd, *J* = 5.7, 3.8 Hz, 2H), 3.87 (dd, *J* = 5.7, 3.8 Hz, 2H), 3.74 – 3.53 (m, 50H), 3.37 (s, 3H). ^{13}C NMR (101 MHz, $CDCl_3$) δ 170.57, 163.23, 132.36, 122.34, 114.46, 72.11, 71.08, 70.82, 70.78, 70.74, 70.68, 69.72, 67.80, 59.23.

Scheme S2: Conditions for Synthesis of **4** from **3** (avg. n = 11-12)

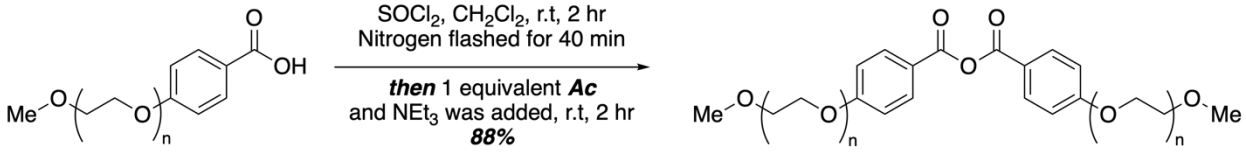

Anhydride 4 (An)

$SOCl_2$ (392 mg, 3.3 mmol) was added to a stirred solution of **Ac** (958 mg, 1.43 mmol) in dichloromethane (8 mL) at room temperature. After 2 hours, the reaction was dried by flushing with nitrogen for 40 min. At that point, (353 mg, 3.5 mmol) NEt_3, and **Ac** (958 mg, 1.43 mmol) in dichloromethane (8 mL) were added to the reaction at room temperature. After 2 h, the reaction was concentrated under reduced pressure, redissolved in toluene, and the solid particles filtered out. The filtrate was concentrated under reduced pressure and purified via flash chromatography (15 × 1.2 cm, dichloromethane to 1:10 acetone/dichloromethane) to afford anhydride **4** (An) as white solid (1.7 g, 88%). ^{1}H NMR (400 MHz, $CDCl_3$) δ 8.11 – 8.07 (m, 4H), 7.02 – 6.99 (m, 4H), 4.24 – 4.20 (m, 4H), 3.91 – 3.88 (m, 4H), 3.75 – 3.61 (m, 120H), 3.56 – 3.54 (m, 6H), 3.38 (s, 8H). ^{13}C NMR (101 MHz, $CDCl_3$) δ 164.00, 162.41, 132.98, 121.52, 114.87, 72.09, 71.07, 70.85, 70.79, 70.77, 70.73, 70.68, 69.63, 67.93, 59.22.

Polymer poly(DMAm$_{70}$-AA$_{30}$)

Poly(DMAm$_{70}$-AA$_{30}$) was synthesized by reversible addition fragmentation chain transfer (RAFT) polymerization using acrylic acid (1.000 g, 13.887 mmol) as the carboxylic-acid-containing monomer, *N*,*N*-dimethylacrylamide (3.209 g, 32.38 mmol) as an inert backbone-forming monomer, 2,2′-azobis[2-(2-imidazolin-2-yl)propane]dihydrochloride (VA-044) as the radical initiator (0.030 g, 0.093 mmol), and 2-(((ethylthio)-carbonothioyl)thio)propionic acid (PAETC) (0.097 g, 0.46 mmol) as the chain transfer agent. All were added to a round bottom flask (50 mL). Water 8.0 mL) was used as the solvent in a ratio of 1:2 (total weight of chemicals to water). The solution was sonicated for 5 min. The resulting reaction mixture was purged with argon for 20 min to deoxygenate and then placed in an oil bath at 45 °C for 16 h. ^{1}H NMR spectroscopy was used to determine the conversion of monomers to be >95%. The crude product was precipitated in

acetone and dried under reduced pressure at 30 °C for 24 h. The network was synthesized with 100 total monomer units in the primary chain, 30% AA and 70% DMAm.
GPC results show well-controlled polymerization. A dispersity of 1.2 and an M_n of 5937 were observed.

2. Reaction Setup and Monitoring

mEDC and Pyridine System

This procedure was used for the datasets in Figure 1. Pyridine (Py) or a derivative (4-methylpyridine (MePy) or 4-methoxypyridine (MeOPy)) was weighed into a 10 mL beaker. Internal standard N,N-dimethylacetamide (DMA) was added to this container, enough to reach a concentration of 75 mM once it is diluted in the NMR tube. Then, ~3 mL of D_2O was added and the solution brought to pD 5.5 with DCl/NaOD. The pD was calculated from the pH probe's reading plus .4.[1] The solution was brought to 5 mL in a volumetric flask. This pyridine/DMA stock solution was reused for multiple experiments. In a vial, the appropriate mass of carbodiimide was measured so that it would be the desired concentration when diluted by 3× in the NMR tube. A blank for locking/shimming was made by combining 400 μL of the DMA/pyridine solution with 200 μL of D_2O. Once the 500 MHz NMR was set up using the blank, 400 μL of the DMA/pyridine solution was added to the NMR tube. The carbodiimide was dissolved in 1 mL D_2O and 200 μL of this solution were added to the DMA/pyridine solution. The time that the two solutions were combined was noted, then the solution was mixed and inserted into the NMR probe. Single scans with a 15 s delay were taken every 30 s for the duration of the experiment. The data was processed using Bruker Topspin 4.1.4 and DynamicsCenter 2.8.2.

Ac System with Pyridines, mEDC, DMA, Ac

Premixing. This procedure was used with the datasets in Figure 2 and involved pre-combining the mEDC and pyridines to maximize the adduct concentration.
Pyridine (Py, MePy, or MeOPy) was weighed into a 10 mL beaker. It was brought to pD 5.5 with a pH probe and DCl/NaOD. In a separate 10 mL beaker was added Ac then internal standard N,N-dimethylacetamide (DMA) (by mass). Then, 3 mL of D_2O was added and the solution was brought to pD 5.5 with a pH probe and DCl/NaOD. The Ac/DMA stock solution was brought to 5 mL in a volumetric flask. This solution was re-used for multiple experiments. In a vial, a mass of carbodiimide was measured so that it would reach the desired concentration when diluted by 3× in the NMR tube. A blank was prepared using 400 μL of the Ac/DMA solution and 200 μL of D_2O. Once the 500 MHz NMR was tuned and shimmed using the blank, 500 μL of the pyridine solution were added to the carbodiimide. It was mixed and allowed to sit for the ideal amount of time for the adduct concentration to peak (N/A for Py, 2.5 min for MePy, and 5 min for MeOPy). Once this premixing stage was done, 400 μL of the DMA/Ac solution was added to 200 μL of the pyridine/carbodiimide solution. The time that the two solutions were combined was noted, then the solution was mixed and inserted into the NMR probe. Single scans with a 15 s delay were taken every 30s for the duration of the experiment. The data was processed using Topspin 4.1.4 and DynamicsCenter 2.8.2.
Many concentrations in kinetic runs were determined by scaling before analysis. To scale these data, each integral for a set of species that interconvert (carbodiimide, adduct, and urea; acid, anhydride, and side product) was summed and the fraction of the total integral value that each species' integral represented was multiplied by a concentration calculated from the initial mass

measured on a balance. We did this because the systems are typically analyzed in bulk, that is, with several runs with different starting concentrations. Errors in the concentration of the internal standard tended to be larger than errors in weighing out the reagents. The internal standards were still used as a second check on the concentrations determined by NMR and to ensure that there was no unaccounted for loss of material (through the production of unassigned byproducts). All systems that were treated using these methods are disclosed in the figure captions.

No Premixing. This procedure was used with the datasets we used to derive rate constants, found in Figures S39-70 below. We did not pre-combine the mEDC and pyridines to maximize the adduct concentration so that we could observe adduct formation in the MePy and MeOPy datasets.
Pyridine (Py, MePy, or MeOPy) was weighed into a 10 mL beaker. Ac was added to the beaker then DMA (by mass). Then, 3 mL of D_2O was added and the stock solution was brought to pD 5.5 with a pH probe and DCl/NaOD. The stock solution was brought to 5 mL in a volumetric flask. This solution was re-used for multiple experiments. In a vial, a mass of carbodiimide was measured so that it would reach the desired concentration when diluted by 3× in the NMR tube. A blank was prepared using 400 μL of the stock solution and 200 μL of D_2O. Once the 500 MHz NMR was tuned and shimmed using the blank, 400 μL of the stock solution was added to 200 μL of the carbodiimide solution, created as soon before the experiment as possible by adding 1 mL D_2O to the carbodiimide. The time that the two solutions were combined was noted, then the solution was agitated and then inserted into the NMR probe. Single scans were taken every 15 s for the duration of the experiment. The data was processed using Topspin 4.1.4 and DynamicsCenter 2.8.2.

Anhydride Decomposition for Side Product Identification
MeOPy was weighed into a 10 mL beaker. 1 mL D_2O was added and the stock solution was brought to pD 5.5 with a pH probe and DCl/NaOD. The stock solution was brought to 2 mL in a volumetric flask. In a vial, the anhydride derived from Ac (An) was measured so that it would reach 25 mM when diluted by 1.5× in the NMR tube. Once ready to start the 500 MHz NMR acquisition, 200 μL of the MeOPy stock solution was added to the An, then mixed and added to the NMR tube. The time that these solutions were combined was noted. The An vial was rinsed with 400 μL D_2O, which was then added to the NMR tube. The solution was agitated then inserted into the NMR probe. Single scans were taken every 15 s for the duration of the experiment. The data was processed using Topspin 4.1.4.

Transient Hydrogel
Rheology. The polymer solution was prepared by dissolving poly($DMAm_{70}$-AA_{30}) (1.0 g) in deionized water (0.9 mL). The solution was then brought to pH 5.5 with pH paper. A MeOPy solution was prepared at pH 5.5 using a pH probe. MeOPy (2.0 M, 0.03 mL) and EDC /mEDC (2.5 M, 0.11 mL) were premixed for 5 min to allow the adduct to peak. The two solutions were then combined in a TA instrument (New Castle, DE) Discovery HR-1 rheometer. The polymer solution (0.25 mL) and distilled water (0.16 mL) were loaded on the Peltier plate of the rheometer using a 1 mL syringe and previously mixed EDC/mEDC and MeOPy solution (0.14 mL) was injected on top of the polymer layer also using a 1 mL syringe. Mixing of polymer and EDC solutions was achieved through rheometer oscillation. Storage and loss moduli during gelation and hydrolysis processes were monitored during time sweep experiments at 20 °C using an angular frequency of 10 rad/s at 1% strain.

3. NMR Spectra of Synthesized Compounds

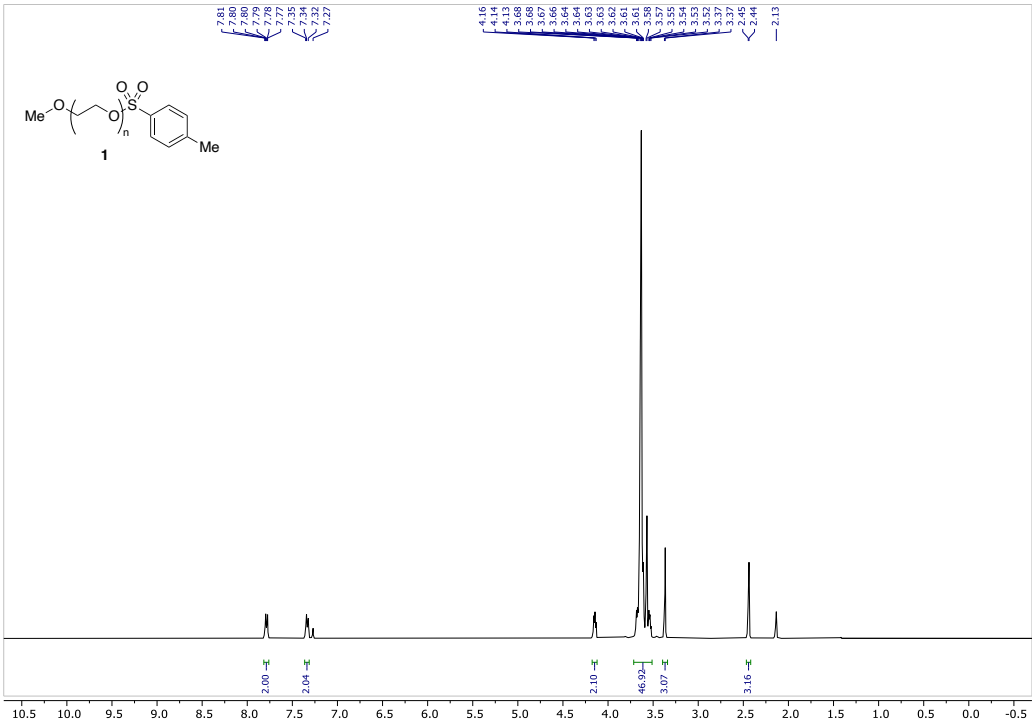

Figure S1: NMR spectra of purified tosylated PEG-550 **1** (avg. n = 11-12)

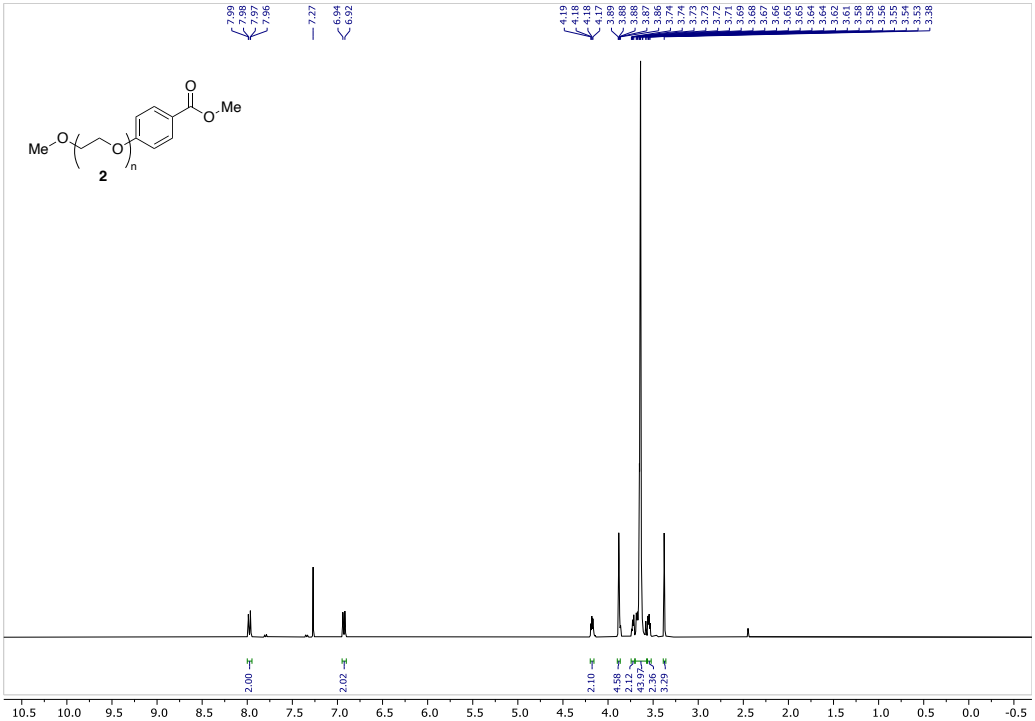

Figure S2: NMR Spectrum of purified **2** (avg. n = 11-12)

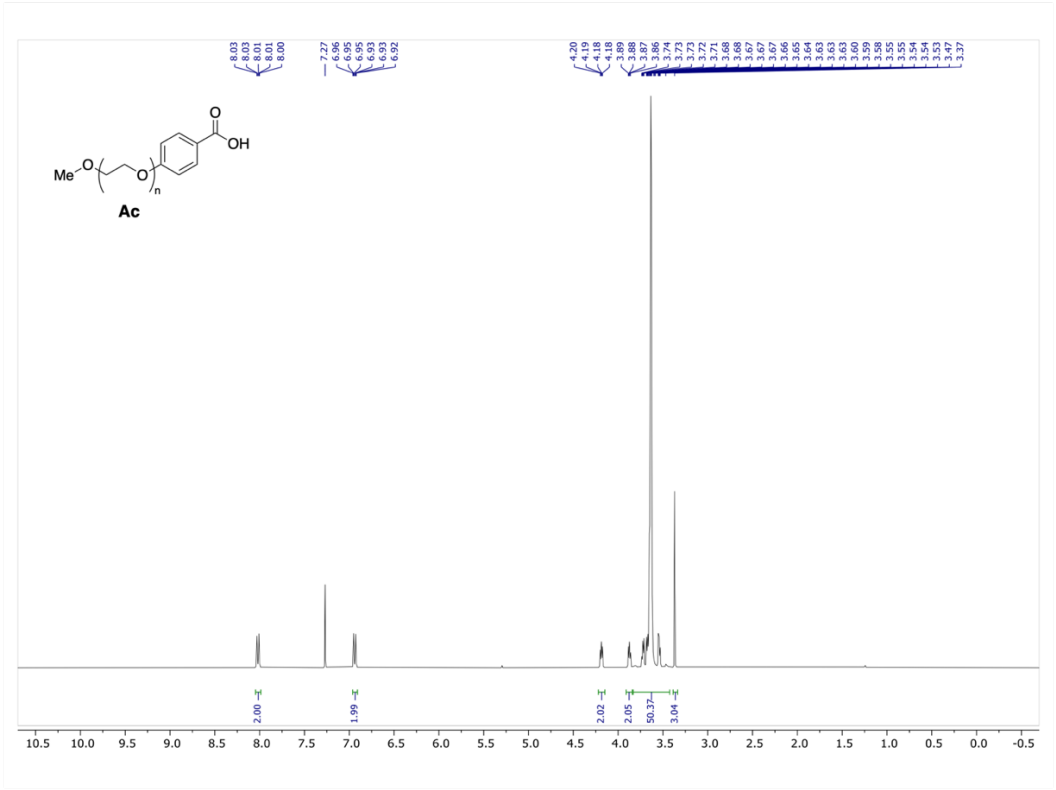

Figure S3: ^{1}H NMR spectrum of purified **Ac** (avg. n = 11-12)

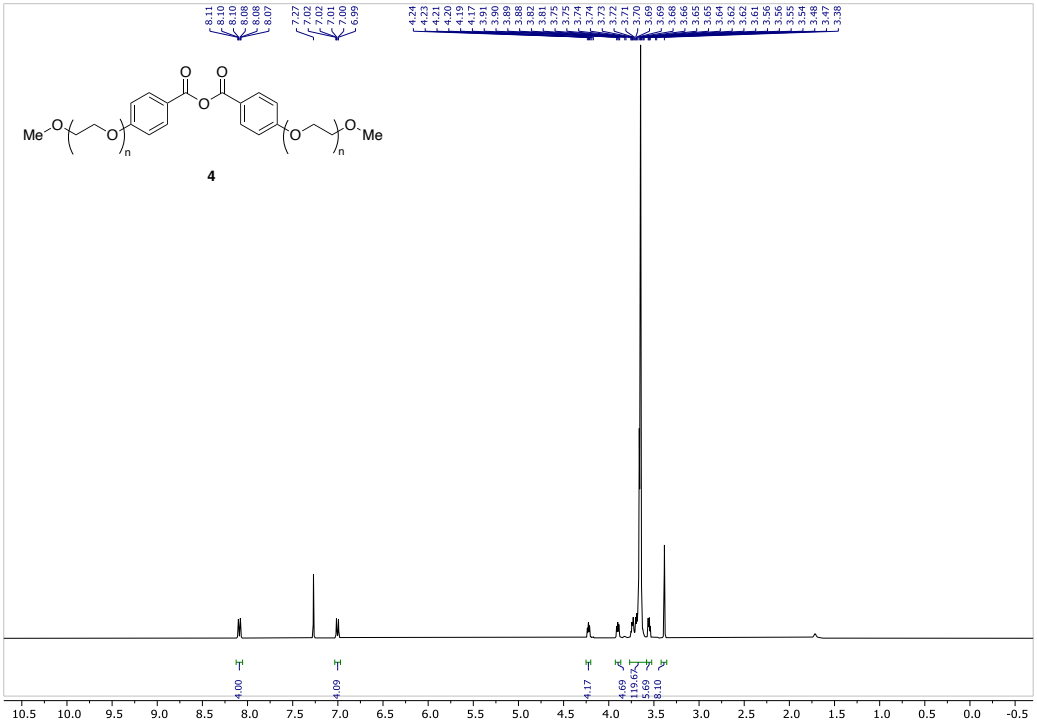

Figure S4: ^{1}H NMR spectrum of purified anhydride **4** (avg. n = 11-12)

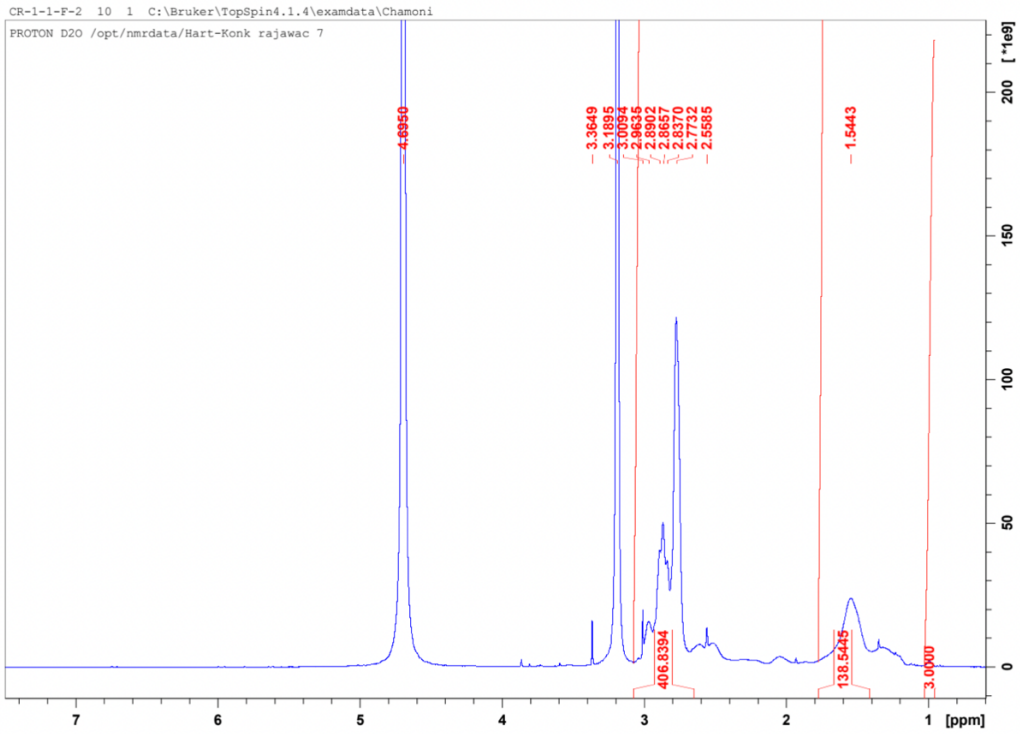

Figure S5: Polymer poly(DMAm$_{70}$-AA$_{30}$) NMR shows no vinyl peaks (around 6 ppm). This confirms that the synthesis of the hydrogel was accomplished with full conversion.

4. Typical Spectra for Kinetics Runs

mEDC/Pyridine system

This is the 300 mM pyridine (Py) adduct system in Figure 1. It contains 300 mM Py with 75 mM mEDC, 75 mM N,N-dimethylacetamide (DMA) as an internal standard in D_2O at pD 5.5 at the start of the experiment. NMR spectra at two chemical shift ranges over a variety of times are shown in Figures S6 and S7.

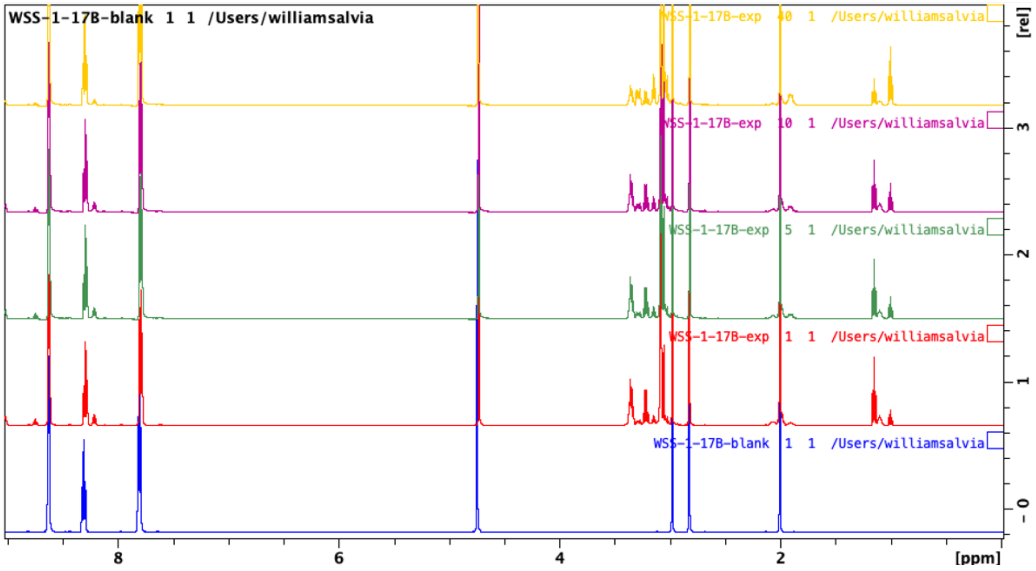

Figure S6: A set of NMR spectra containing every visible signal at a variety of timestamps for 300 mM Py with 75 mM mEDC, 75 mM DMA in D_2O at pD 5.5. The blank (bottom spectrum) did not contain the mEDC. From bottom to top, these scans were taken at .55 min, 2.55 min, 5.07 min, and 20.13 min from the addition of the MeOPy solution to the mEDC solution in the NMR tube. The signals used for identification are mEDC at ~1.15 ppm, mEDU at ~1.0 ppm, and the adduct at ~1.09, ~7.6, and ~8.7 ppm. The chemical shifts are calibrated to DMA at 2.08 ppm.

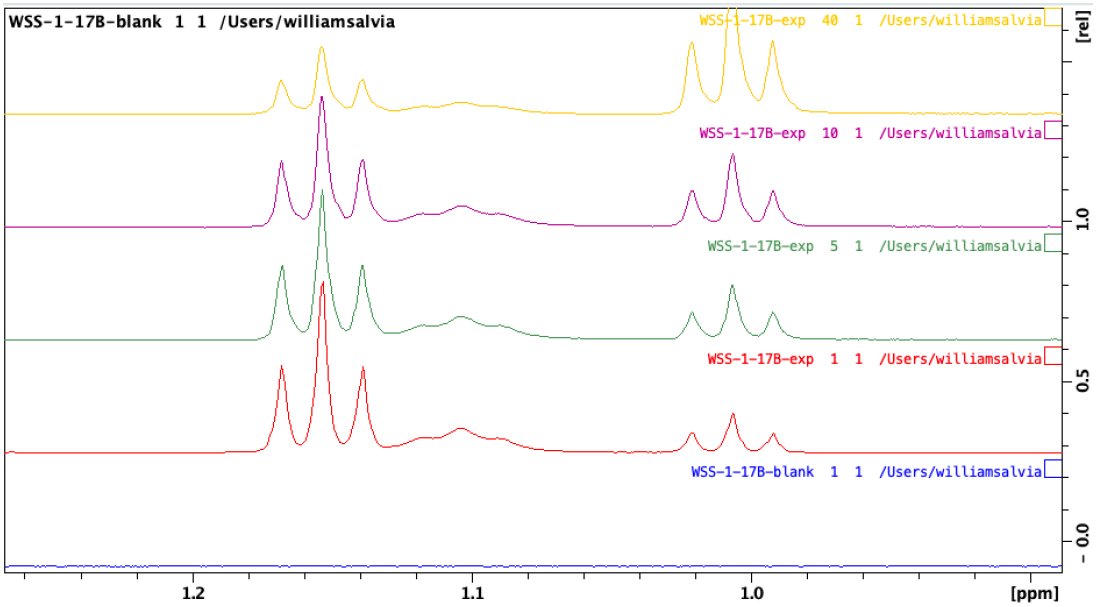

Figure S7: The same spectra as Figure S6 zoomed in on the mEDC (~1.15 ppm), adduct (~1.09 ppm), and mEDU (~1 ppm) signals.

The NMR signals for the new species are consistent with addition of the pyridine to the carbodiimide, as is the MS data (Figure S12).

Ac System

mEDC. This is the 300 mM MeOPy mEDC system in Figure 2. It contains 300 mM MeOPy, 100 mM mEDC, 75 mM DMA as an internal standard, 50 mM Ac at the start of the experiment. NMR spectra at two chemical shift ranges over a variety of times are shown in Figures S8 and S9.

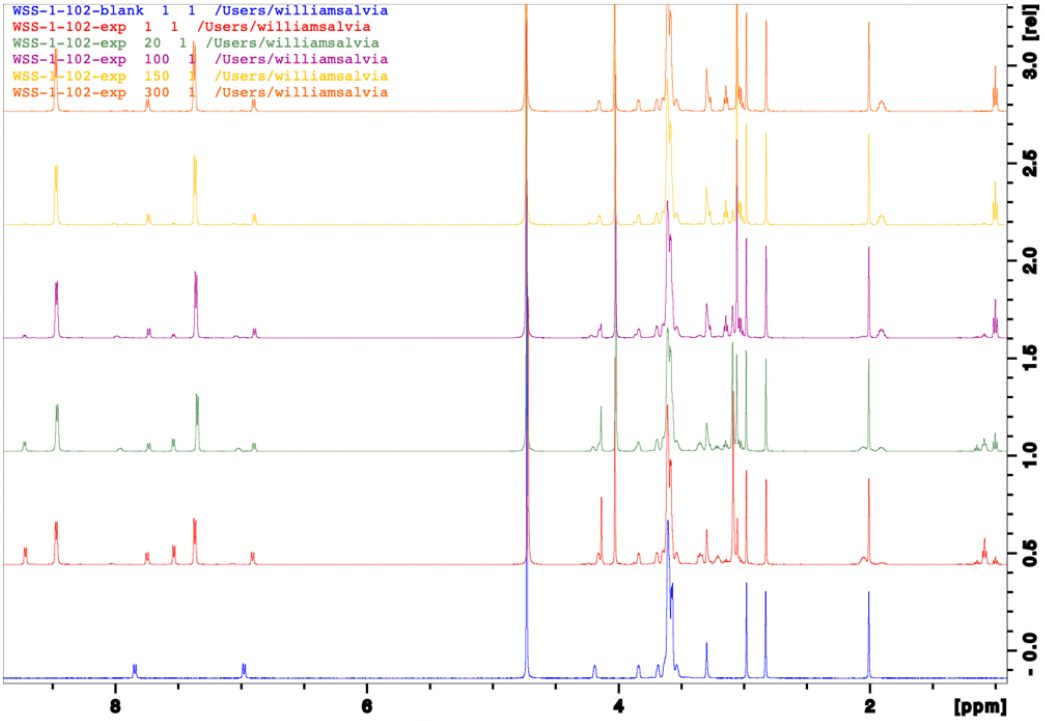

Figure S8: A set of NMR spectra containing every visible signal at a variety of timestamps for 300 mM MeOPy with 100 mM mEDC, 50 mM Ac, and 75 mM DMA in D_2O at pD 5.5. The blank (bottom spectrum) did not contain the mEDC. From bottom to top, these scans were taken at 1.03 min, 9.38 min, 42.83 min, 63.71 min, and 125.98 min from the combination of the MeOPy/mEDC premixed solution and the Ac/DMA solution. The signals used for identification are mEDC at ~1.15 ppm, mEDU at ~1.0 ppm, the adduct at ~1.09, ~7.75, and ~6.91 ppm, Ac at ~7.5 and ~8.7 ppm and the anhydride at ~8.03 and ~7.07 ppm. The chemical shifts are calibrated to DMA at 2.08 ppm.

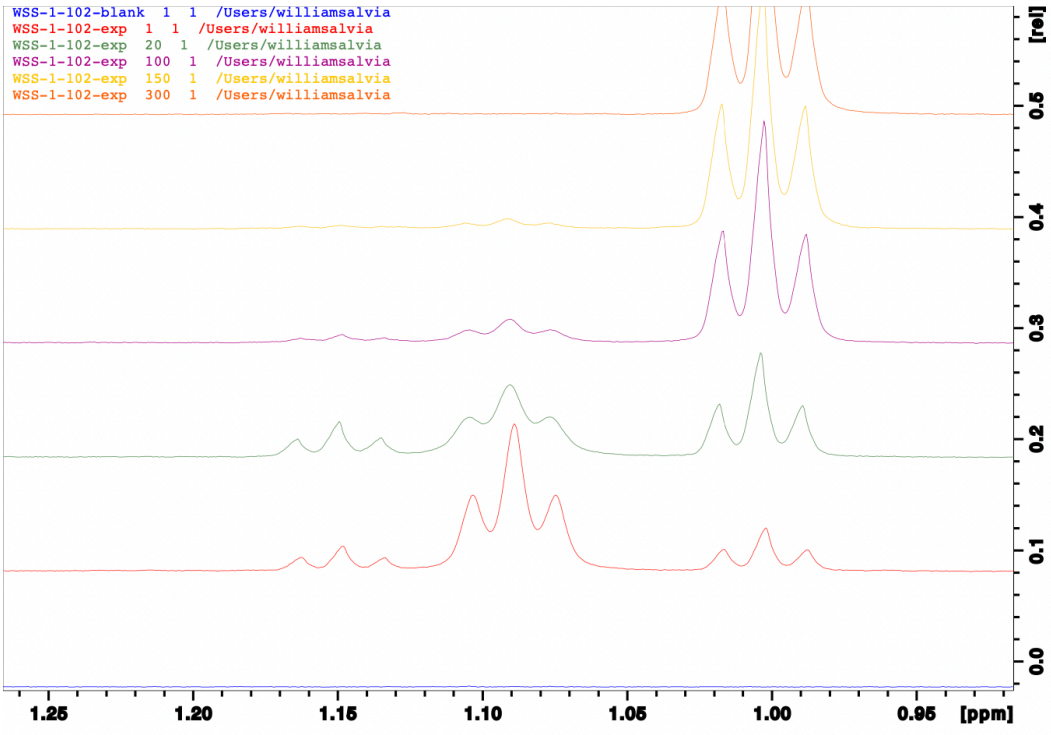

Figure S9: The same spectra as Figure S8 zoomed in on the mEDC (~1.15 ppm), adduct (~1.09 ppm), and mEDU (~1 ppm) signals.

EDC. This is the 300 mM MeOPy EDC system in Figure 2. It contains 300 mM MeOPy, 100 mM EDC, 75 mM DMA as an internal standard, and 50 mM Ac at the start. NMR spectra at two chemical shift ranges over a variety of times are shown in Figures S10 and S11.

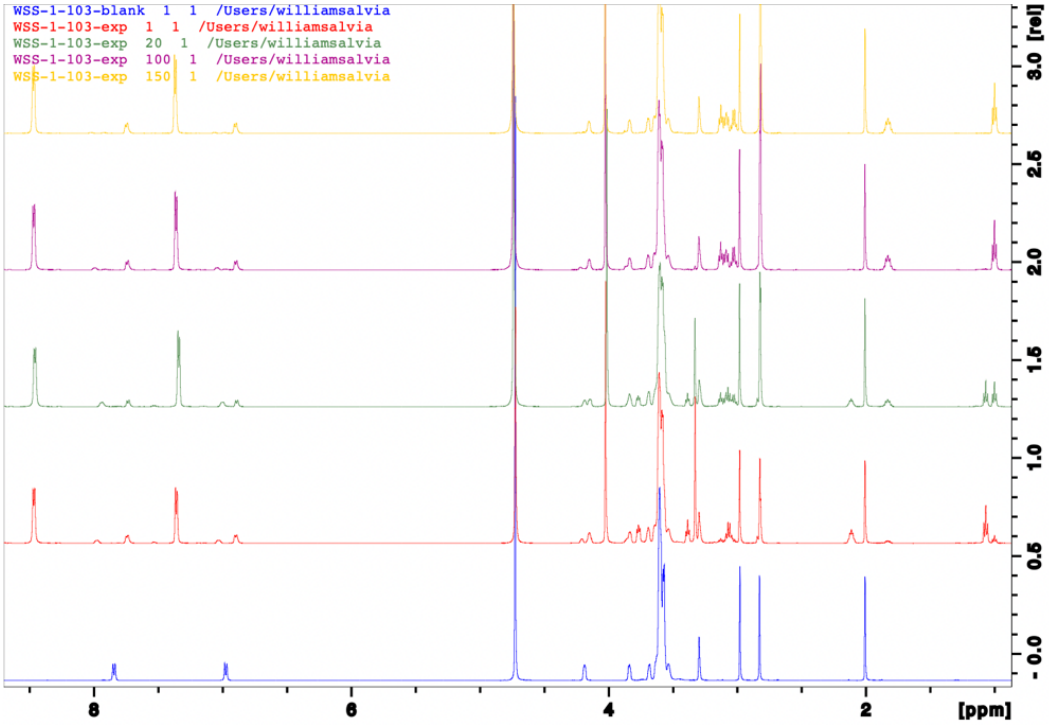

Figure S10: A set of NMR spectra containing every visible signal at a variety of timestamps for 300 mM MeOPy with 100 mM EDC, 50 mM Ac, and 75 mM DMA in D_2O at pD 5.5. The blank (bottom spectrum) did not contain the EDC. From bottom to top, these scans were taken at .93 min, 9.3 min, 42.7 min, and 63.16 min from the combination of the MeOPy/EDC solution and the Ac/DMA solution. The signals used for identification are EDC at ~1.08 ppm, EDU at ~1.0 ppm, Ac at ~6.90 and ~7.74 ppm and the anhydride at ~7.97 and ~7.03 ppm. The chemical shifts are calibrated to DMA at 2.08 ppm.

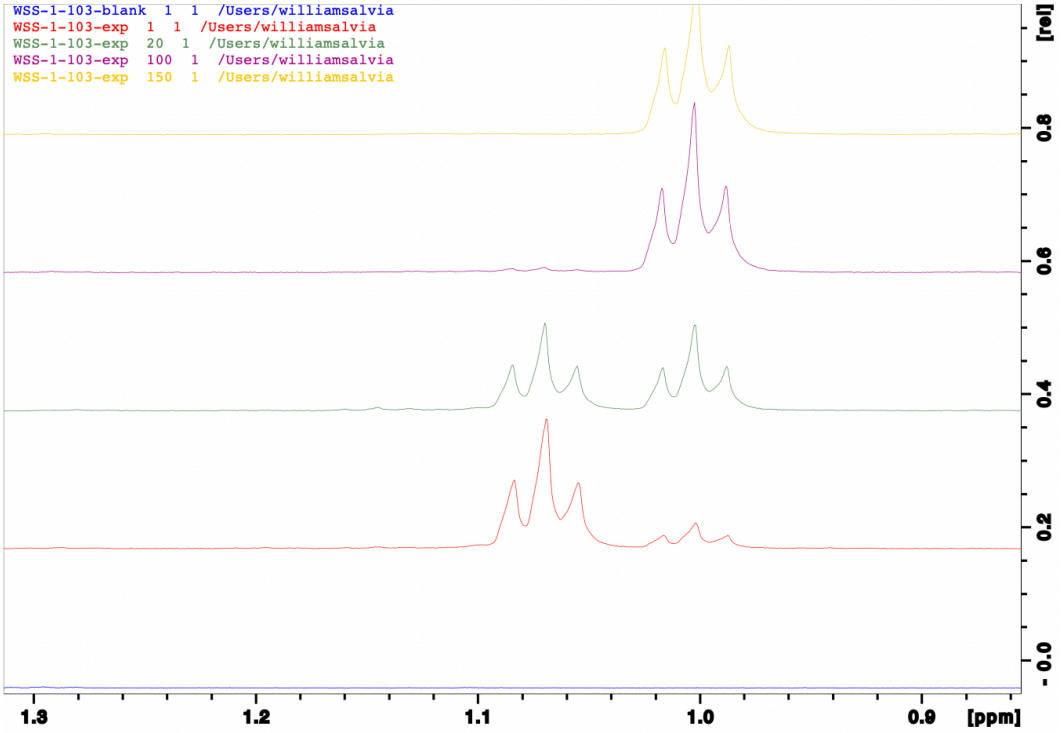

Figure S11: The same spectra as Figure S10 zoomed in on the EDC (~1.08 ppm) and EDU (~1.0 ppm) signals.

5. MS Detection of the Adduct

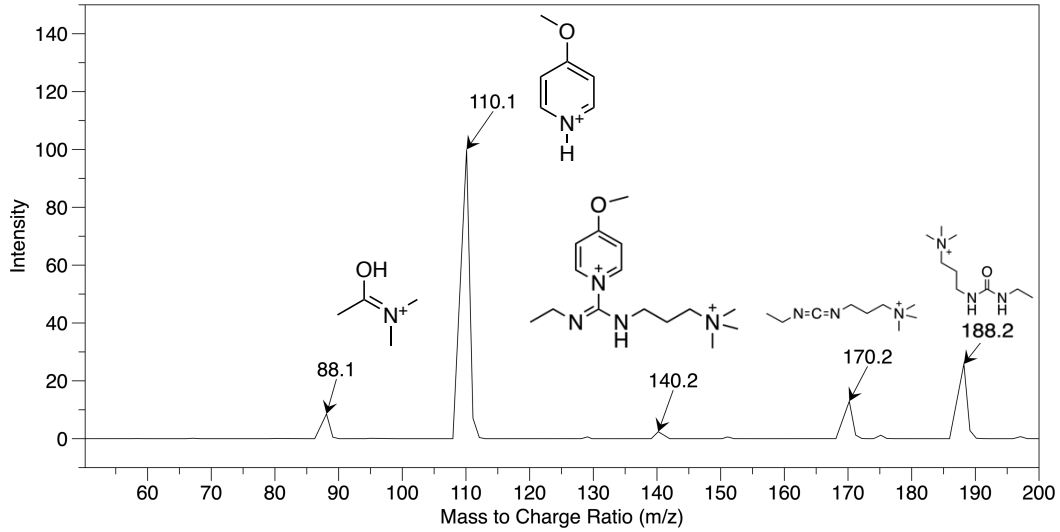

Figure S12: Positive-ion MS spectrum taken with a Bruker Esquire-LC ESI MS instrument of a diluted solution (5 µL diluted with 1 mL water) of 300 mM MeOPy, 75 mM mEDC and 75 mM N,N-dimethylacetamide (DMA). The adduct was allowed to form for ~5 min before dilution. From left to right the species detected are singly ionized DMA (88.1 m/z), singly ionized MeOPy (110.1 m/z), doubly ionized adduct (140.2 m/z), singly ionized mEDC (170.2 m/z), and singly ionized mEDU (188.2 m/z).

6. Data Fitting

mEDC/Pyridine System

The kinetic data for this system was fit to Eq S1-2:

$$\text{Carbodiimide} + \text{Pyridine} \underset{k_{-4}}{\overset{k_4}{\rightleftharpoons}} \text{Adduct} \quad \text{(S1)}$$

$$\text{Carbodiimide} \xrightarrow{k_5} \text{Urea} \quad \text{(S2)}$$

Therefore, it is described by these differential equations (Eq S3-6), where E is mEDC, B is the adduct, U is the urea byproduct, and P is the pyridine:

$$\frac{d[E]}{dt} = -k_4[E][P] - k_5[E] + k_{-4}[B] \quad \text{(S3)}$$

$$\frac{d[B]}{dt} = k_4[E][P] - k_{-4}[B] \quad \text{(S4)}$$

$$\frac{d[U]}{dt} = k_5[E] \quad \text{(S5)}$$

$$\frac{d[P]}{dt} = -k_4[E][P] + k_{-4}[B] \quad \text{(S6)}$$

Ac System

The kinetic data for this system was fit to Eq S7-12, which are the same as Eq 3-8:

$$\text{Acid} + \text{Carbodiimide} \xrightarrow{k_1} \textit{O}\text{-Acylisourea} \quad \text{(S7)}$$

$$\textit{O}\text{-Acylisourea} + \text{Pyridine} \xrightarrow{k_{\text{fast}}} \text{Acylpyridinium} + \text{Urea} \quad \text{(S8)}$$

$$\text{Acylpyridinium} + \text{Acid} \underset{k_{-2}}{\overset{k_2}{\rightleftharpoons}} \text{Anhydride} + \text{Pyridine} \quad \text{(S9)}$$

$$\text{Acylpyridinium} \xrightarrow{k_3} \text{Acid} + \text{Pyridine} \quad \text{(S10)}$$

$$\text{Carbodiimide} + \text{Pyridine} \underset{k_{-4}}{\overset{k_4}{\rightleftharpoons}} \text{Adduct} \quad \text{(S11)}$$

$$\text{Carbodiimide} \xrightarrow{k_5} \text{Urea} \quad \text{(S12)}$$

Therefore, it is described by these differential equations Eq S13-18, where Ac is the aforementioned acid Ac, E is the carbodiimide, B is the adduct, U is the urea byproduct, An is the anhydride, P is the pyridine (with or without electron-donating substituents), I is the acylpyridinium intermediate, and O is the O-acylisourea intermediate:

$$\frac{d[Ac]}{dt} = -k_1[Ac][E] + k_{-2}[An][P] + k_3[I] - k_2[I][Ac] \quad \text{(S13)}$$

$$\frac{d[E]}{dt} = -k_1[Ac][E] - k_4[E][P] + k_{-4}[B] - k_5[E] \quad \text{(S14)}$$

$$\frac{d[B]}{dt} = k_4[E][P] - k_{-4}[B] \quad \text{(S15)}$$

$$\frac{d[U]}{dt} = k_5[E] + k_{fast}[O][P] \quad \text{(S16)}$$

$$\frac{d[An]}{dt} = k_2[I][Ac] - k_{-2}[An][P] \quad \text{(S17)}$$

$$\frac{d[P]}{dt} = -k_4[E][P] - k_{fast}[O][P] + k_{-4}[B] - k_{-2}[An][P] + k_2[I][Ac] + k_3[I] \quad \text{(S18)}$$

Assuming the steady-state approximation for the O-acylisourea, we derive Eq S19.

$$[O] = \frac{k_1[Ac][E]}{k_{fast}[P]} \quad \text{(S19)}$$

Assuming the steady state approximation for the acylpyridinium, we derive Eq S20.

$$[I] = \frac{k_{fast}[O][P]+k_{-2}[An][P]}{k_2[Ac]+k_3} \quad \text{(S20)}$$

If we combine Eq S18 and S19, we derive Eq S21.

$$[I] = \frac{k_1[Ac][E]+k_{-2}[An][P]}{k_2[Ac]+k_3} \quad \text{(S21)}$$

To simplify future expressions, we'll simplify Eq S21 to Eq S22, where p is Eq S23 and, therein, $\alpha = k_2/k_3$.

$$[I] = \frac{1}{k_3}p \quad \text{(S22)}$$

$$p = \frac{k_1[Ac][E]+k_{-2}[An][P]}{\alpha[Ac]+1} \quad \text{(S23)}$$

Therefore, Eq S13, S16, S17, and S18 can be rewritten as Eq S24, S25, S26, and S27.

$$\frac{d[Ac]}{dt} = -k_1[Ac][E] + k_{-2}[An][P] - \alpha[Ac]p + p \quad \text{(S24)}$$

$$\frac{d[U]}{dt} = k_5[E] + k_1[Ac][E] \quad \text{(S25)}$$

$$\frac{d[An]}{dt} = \alpha[Ac]p - k_{-2}[An][P] \quad \text{(S26)}$$

$$\frac{d[P]}{dt} = -k_1[Ac][E] - k_4[E][P] + k_{-4}[B] - k_{-2}[An][P] + \alpha[Ac]p + p \quad \text{(S27)}$$

Both models were fit using "kinmodel", a kinetics program first published in the Supporting Information of this publication: J. Org. Chem. 2020, 85, 682–690.[2]

7. Calculations

pKa in D_2O

According to Krężel & Bal,[3] the difference in pKa (ΔpK^{D-H}) measured in a ^1H_2O solution (pK^H) and a D_2O solution (pK^D) are expressed by Eq S28 and S29.

$$\Delta pK^{D-H} = 0.076\ pK^H - 0.05 \quad \text{(S28)}$$

$$pK^{D-H} = pK^D - pK^H \quad \text{(S29)}$$

which can be rearranged to Eq S30 to find pK^D.

$$pK^D = pK^{D-H} + pK^H \quad \text{(S30)}$$

The pK^H values of Py, MePy and MeOPy are 5.23, 5.99, and 6.58, respectively.[4] Eq S31, S33, and S35 use Eq S28 to find ΔpK^{D-H} values, and we used Eq S32, S34, and S36 to find pK^D with Eq S29.

$$\text{Py: } \Delta pK^{D-H} = 0.076\ pK^H - 0.05 = 0.076\ (5.23) - 0.05 = .35 \quad \text{(S31)}$$

$$\mathbf{pK^D} = .35 + 5.23 = \mathbf{5.58} \quad \text{(S32)}$$

$$\text{MePy: } \Delta pK^{D-H} = 0.076\ pK^H - 0.05 = 0.076\ (5.99) - 0.05 = .41 \quad \text{(S33)}$$

$$\mathbf{pK^D} = .41 + 5.99 = \mathbf{6.40} \quad \text{(S34)}$$

$$\text{MeOPy: } \Delta pK^{D-H} = 0.076\ pK^H - 0.05 = 0.076\ (6.58) - 0.05 = .45 \quad \text{(S35)}$$

$$\mathbf{pK^D} = .45 + 6.58 = \mathbf{7.03} \quad \text{(S36)}$$

Py, MePy, and MeOPy Percent Deprotonated

The Henderson-Hasselbalch equation, Eq S37, was applied with Eq S38 to calculate the percent deprotonation in Eq S39, where P_B and P_{HB^+} are the fraction of each species present in solution.

$$\frac{[B]}{[HB^+]} = 10^{pD - pK^D} \quad \text{(S37)}$$

$$P_B + P_{HB^+} = 1 \quad \text{(S38)}$$

$$\frac{P_B}{1-P_B} = 10^{pD-pK^D} \quad \text{(S39)}$$

Which can be rearranged to Eq S40:

$$P_B = \frac{10^{pD-pK^D}}{1+10^{pD-pK^D}} \quad \text{(S40)}$$

The value used for pKa was the pK^D calculated in Eq S31-36 to determine the percentage of pyridine (Py), 4-methylpyridine (MePy), and 4-methoxypyridine (MeOPy) present in solution at pD 5.5. Eq S41-S43 calculate P_B where B = Py, MePy, and MeOPy, the fraction of pyridine present in solution compared to pyridinium conjugate acid.

$$\mathbf{P_{Py}} = \frac{10^{5.5-5.58}}{1+10^{5.5-5.58}} = .45 = \mathbf{45\%} \quad \text{(S41)}$$

$$\mathbf{P_{MePy}} = \frac{10^{5.5-6.40}}{1+10^{5.5-6.40}} = .11 = \mathbf{11\%} \quad \text{(S42)}$$

$$\mathbf{P_{MeOPy}} = \frac{10^{5.5-7.03}}{1+10^{5.5-7.03}} = .029 = \mathbf{2.9\%} \quad \text{(S43)}$$

Analysis of k_4 with Py, MePy, and MeOPy

Py, MePy, and MeOPy have pK_a's of 5.23, 5.99, and 6.58, respectively,[4] which, when recalculated to account for the difference in behavior of ^{1}H and ^{2}H,[3] become 5.58, 6.40, and 7.03 (Eq S31-S36). This corresponds to 45%, 11%, and 2.9% deprotonated for Py, MePy and MeOPy (Eq S41-43). The presence of roughly 4× more MePy than MeOPy at pD 5.5 is compatible, within the confidence ranges given in Table S2, with a corresponding 4× increase in k_4.

Figure 2 Slopes for mEDC vs EDC

Since the presence of adduct reduces the concentration of pyridine in the system, we needed to ensure that the whole lifetime lengthening effect we observed in Figure 2 was not just due to a effective decreased concentration of MeOPy. To estimate the slope of the second half of the experiment, we chose a timepoint near 30 min and 40 min for both carbodiimides. For EDC, the points were (30.16 min, 7.00 mM) and (40.18 min, 5.08 mM), and for mEDC, the points were (29.88 min, 7.16 mM) and (39.92 min, 5.89 mM). Eqs S44 and S45 show the estimated slopes for each of these experiments.

$$\text{Slope}_{\text{EDC}} = \frac{7.00-5.08\ mM}{30.16-40.18\ min} = \text{-0.192 mM/min} \quad \text{(S44)}$$

$$\text{Slope}_{\text{mEDC}} = \frac{7.16-5.89\ mM}{29.88-39.92\ min} = \text{-0.126 mM/min} \quad \text{(S45)}$$

The ratio of these slopes is described in Eq S46.

$$\text{Slope}_{\text{EDC}}/\text{Slope}_{\text{mEDC}} = \frac{-0.192\ mM/min}{-0.126\ mM/min} = 1.51 \quad \text{(S46)}$$

After the anhydride derived from Ac (An) concentration peaks, EDC's An slope is roughly 50% steeper than mEDC (Eqs S44-S46). This cannot be accounted for by EDC's 25% higher pyridine concentration at the start of the experiment. As the adduct concentration decreases over the course of the experiment, the concentration of mEDC's pyridine approaches EDC's and the difference becomes even less than 25%.

8. Kinetics Experiments

mEDC/Pyridine System

These reactions were completed to identify the rate constants. These fits are derived from Eqs S1-S6. All experiments were completed at room temperature.

Py Plots. Figures S13-S21 contain the model outputs for the Py system (see 7. Data Fitting). All were fit together to yield one set of rate constants. We believe the "Byproduct" is the pyridine adduct (see below).

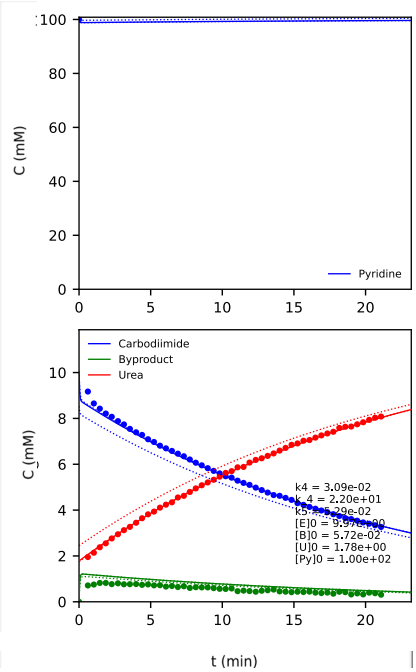

Figure S13: 100 mM Py, 75 mM DMA, 12.5 mM mEDC in D_2O at pD 5.5

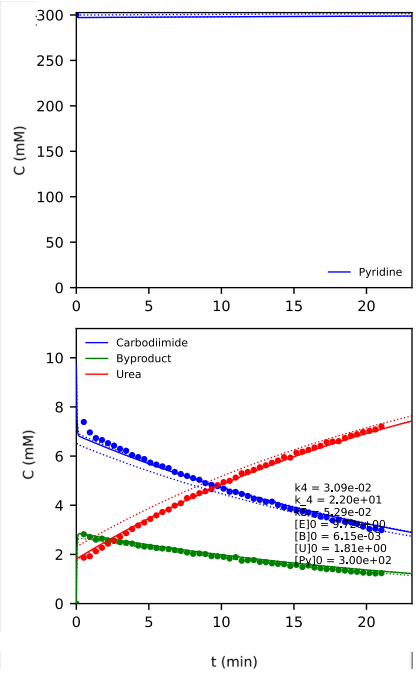

Figure S14: 100 mM Py, 75 mM DMA, 25 mM mEDC in D_2O at pD 5.5

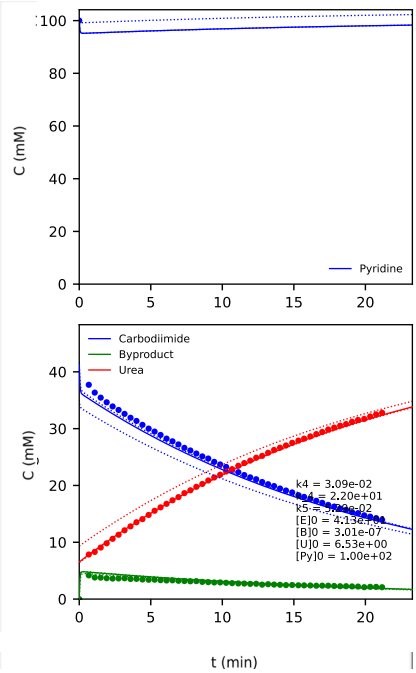

Figure S15: 100 mM Py, 75 mM DMA, 50 mM mEDC in D_2O at pD 5.5

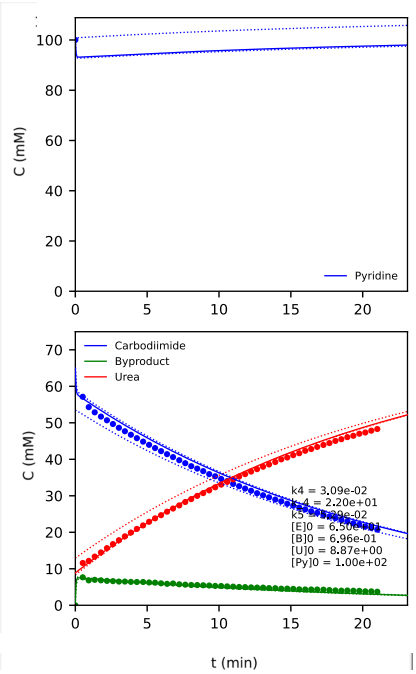

Figure S16: 100 mM Py, 75 mM DMA, 75 mM mEDC in D_2O at pD 5.5

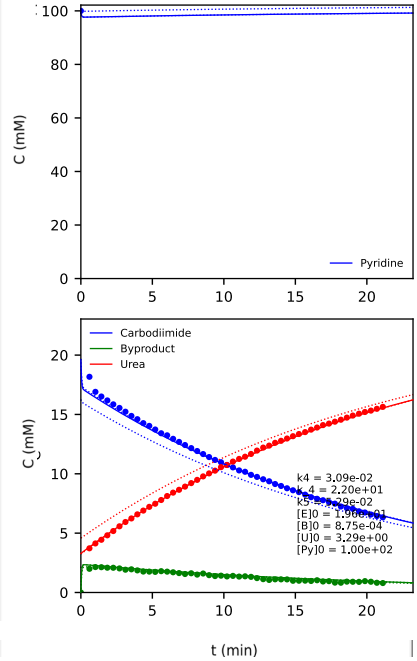

Figure S17: 300 mM Py, 75 mM DMA, 12.5 mM mEDC in D_2O at pD 5.5

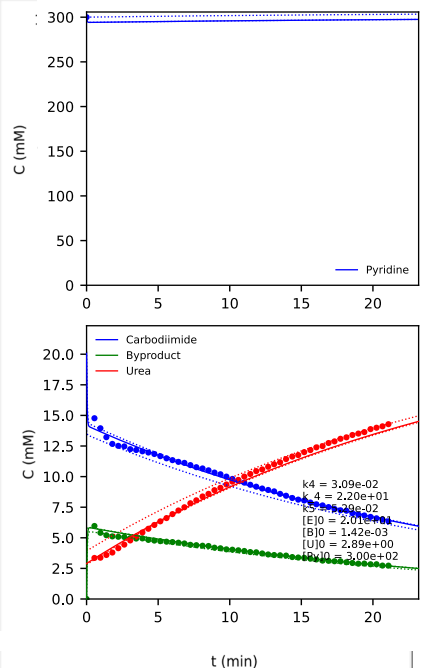

Figure S18: 300 mM Py, 75 mM DMA, 25 mM mEDC in D_2O at pD 5.5

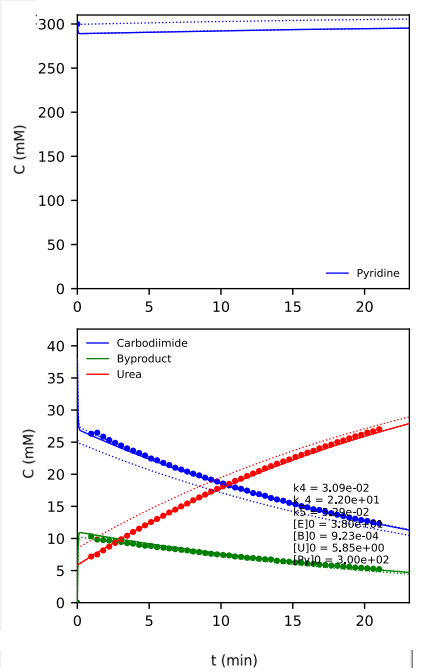

Figure S19: 300 mM Py, 75 mM DMA, 50 mM mEDC in D_2O at pD 5.5

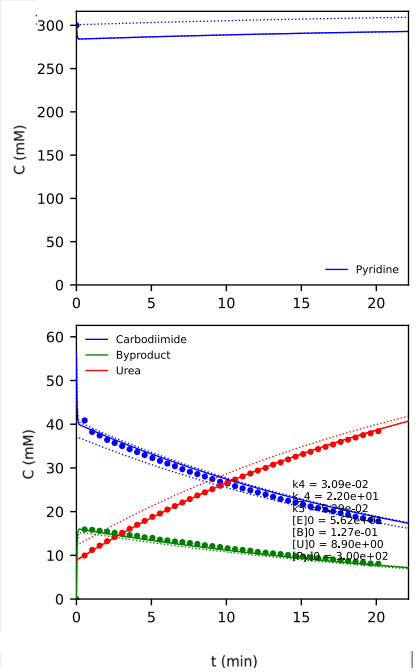

Figure S20: 300 mM Py, 75 mM DMA, 75 mM mEDC in D_2O at pD 5.5

A confidence contour is a visualization of the way that different combinations of values result in a good fit to a model. An ideal confidence contour plot has one spot with high confidence (red, closer to 1). A confidence contour that has an equally good fit over a diagonal line of values means that two parameters are correlated. This means that an infinite number of different combinations of parameter with a certain ratio to one another fit to the model with equal certainty. Confidence contour heat maps in Figure S21 confirmed that the rate constants were constrained, despite k_4 and k_{-4}'s correlation due to Py's fast mechanism.

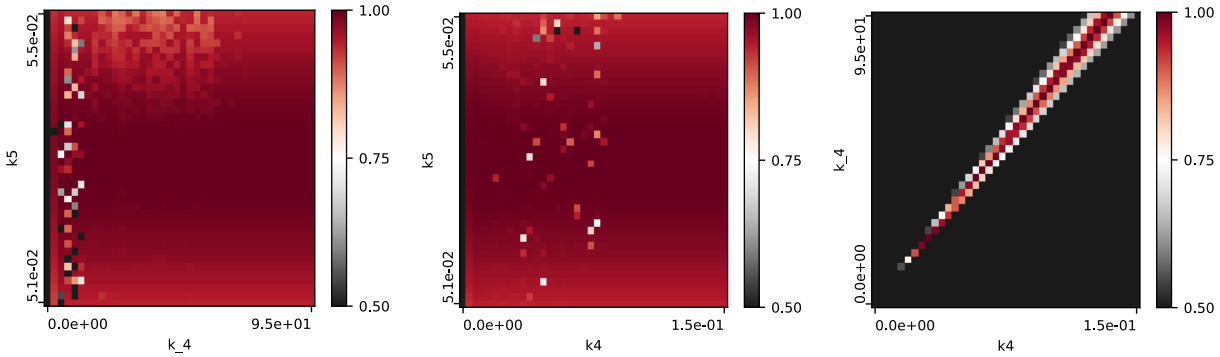

Figure S21: Confidence contours for Py's Adduct Optimization Model. k_4 is in units of mM^{-1} min^{-1}, k_{-4} is in units of min^{-1}, k_5 is in units of min^{-1}.

MePy Plots. Figures S22-S30 contain the kinmodel outputs for the 4-methylpyridine (MePy) system. All were fit together to yield one set of rate constants. We believe the "Byproduct" is the pyridine adduct (see below).

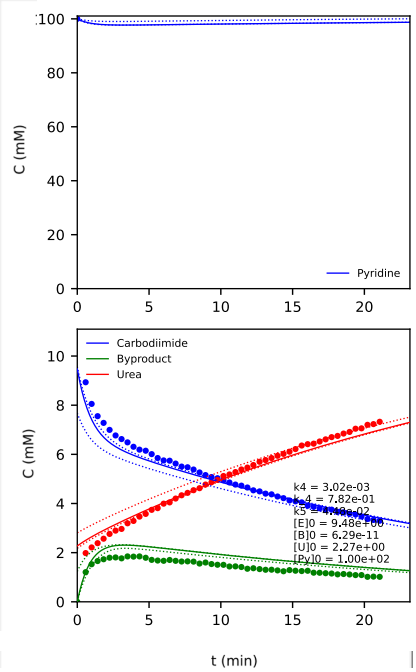

Figure S22: 100 mM MePy, 75 mM DMA, 12.5 mM mEDC in D_2O at pD 5.5

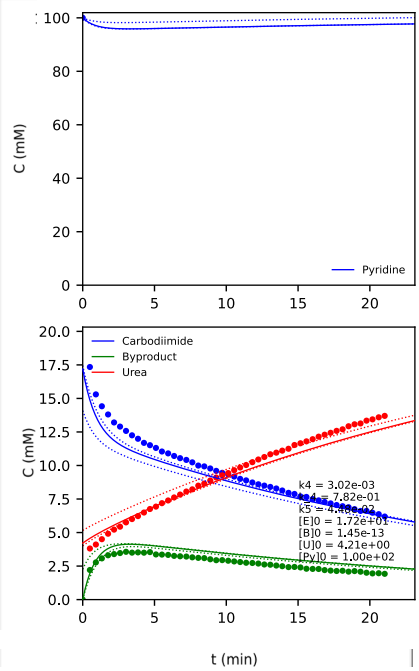

Figure S23: 100 mM MePy, 75 mM DMA, 25 mM mEDC in D_2O at pD 5.5

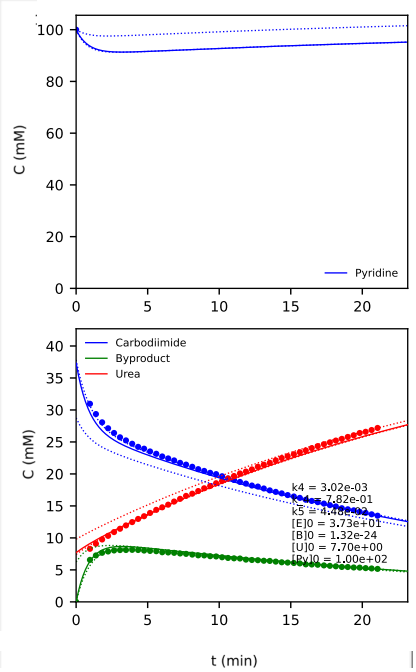

Figure S24: 100 mM MePy, 75 mM DMA, 50 mM mEDC in D_2O at pD 5.5

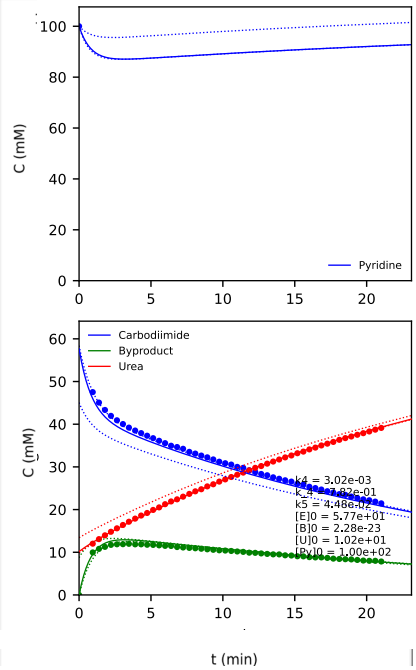

Figure S25: 100 mM MePy, 75 mM DMA, 75 mM mEDC in D_2O at pD 5.5

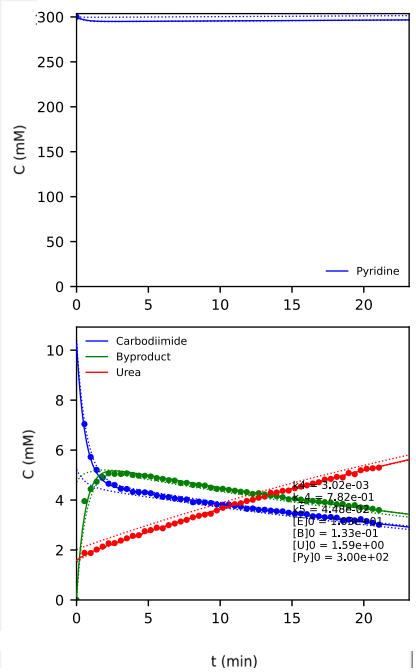

Figure S26: 300 mM MePy, 75 mM DMA, 12.5 mM mEDC in D_2O at pD 5.5

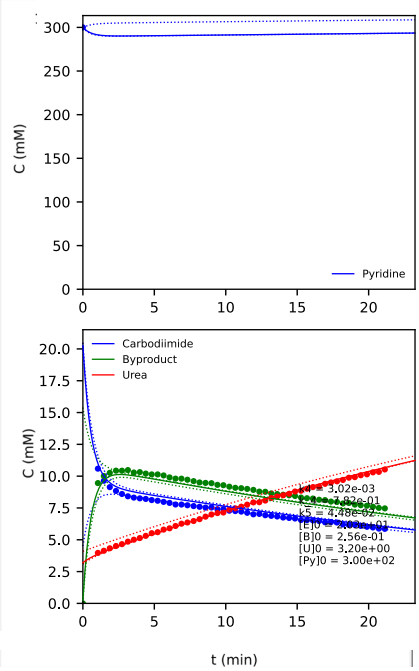

Figure S27: 300 mM MePy, 75 mM DMA, 25 mM mEDC in D_2O at pD 5.5

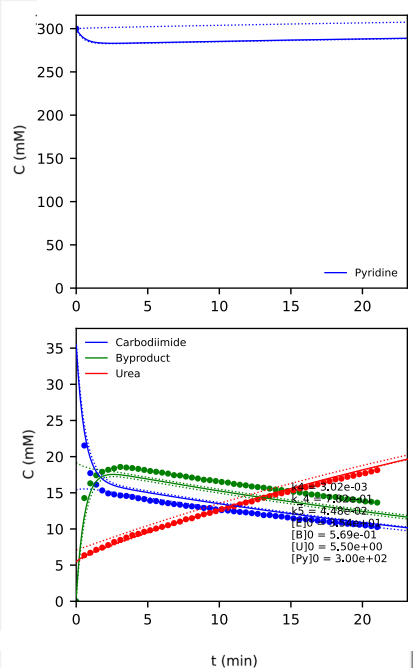

Figure S28: 300 mM MePy, 75 mM DMA, 50 mM mEDC in D_2O at pD 5.5

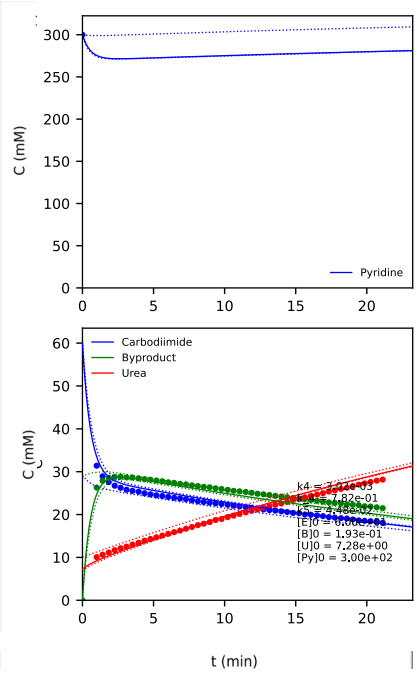

Figure S29: 300 mM MePy, 75 mM DMA, 75 mM mEDC in D_2O at pD 5.5

Confidence contour heat maps confirmed that the rate constants were constrained (Figure S30). For a description of a confidence contour and their utility, see the paragraph above Figure S21.

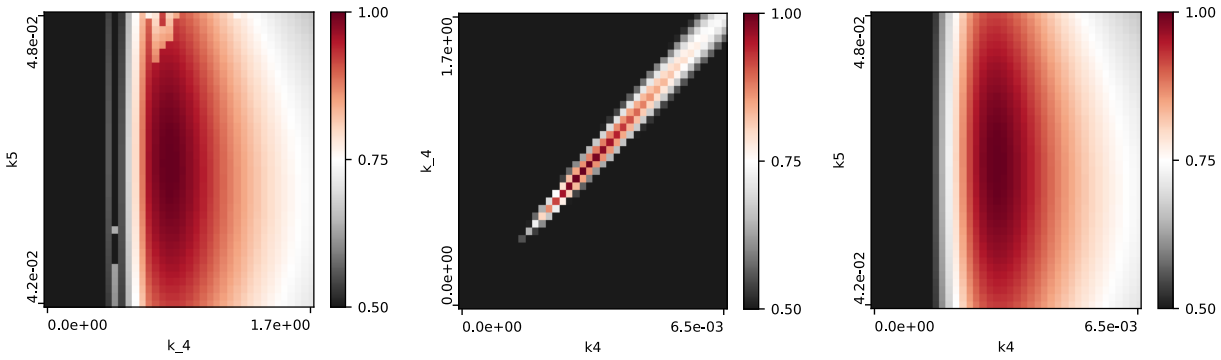

Figure S30: Confidence Contours for MePy Adduct Optimization System. k_4 is in units of mM^{-1} min^{-1}, k_{-4} is in units of min^{-1}, k_5 is in units of min^{-1}.

MeOPy plots. Figures S31-S38 contain the kinmodel outputs for the MeOPy system. All were fit together to yield one set of rate constants. We believe the "Byproduct" is the pyridine adduct (see below).

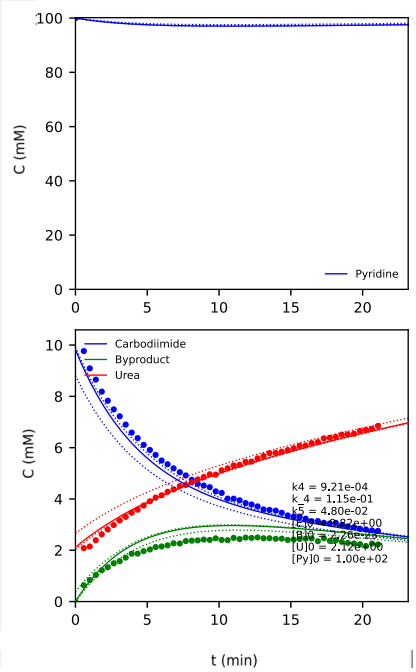

Figure S31: 100 mM MeOPy, 75 mM DMA, 12.5 mM mEDC in D_2O at pD 5.5

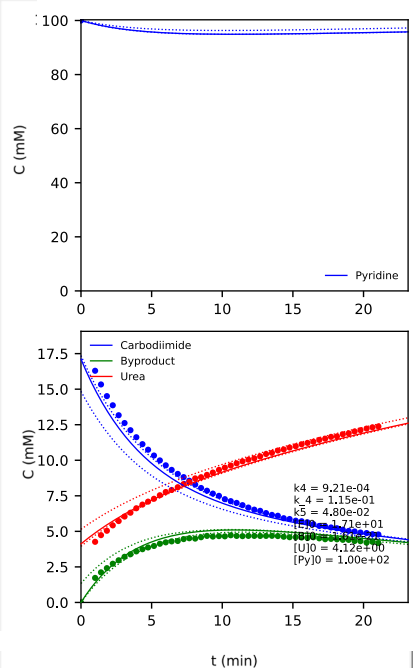

Figure S32: 100 mM MeOPy, 75 mM DMA, 25 mM mEDC in D_2O at pD 5.5

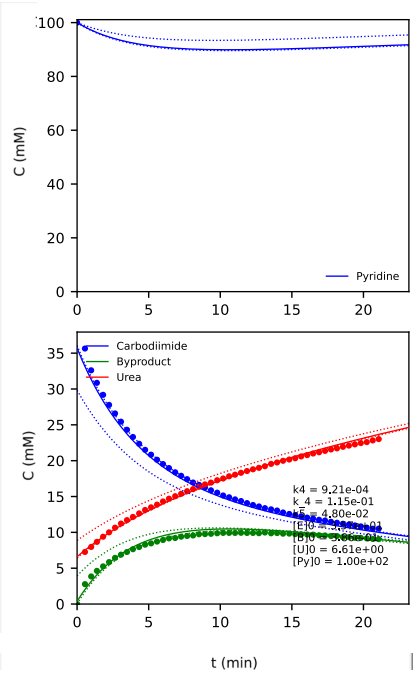

Figure S33: 100 mM MeOPy, 75 mM DMA, 50 mM mEDC in D_2O at pD 5.5

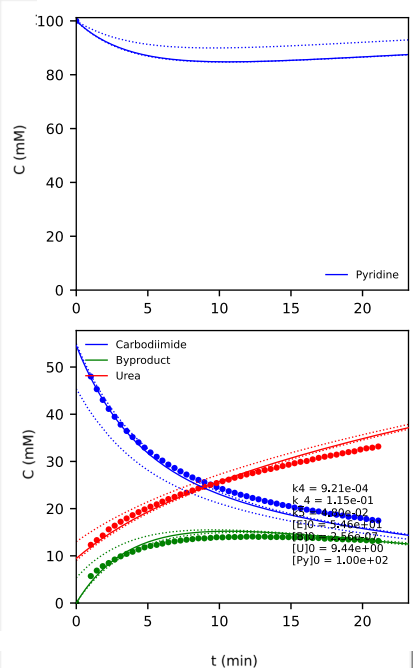

Figure S34: 100 mM MeOPy, 75 mM DMA, 75 mM mEDC in D_2O at pD 5.5

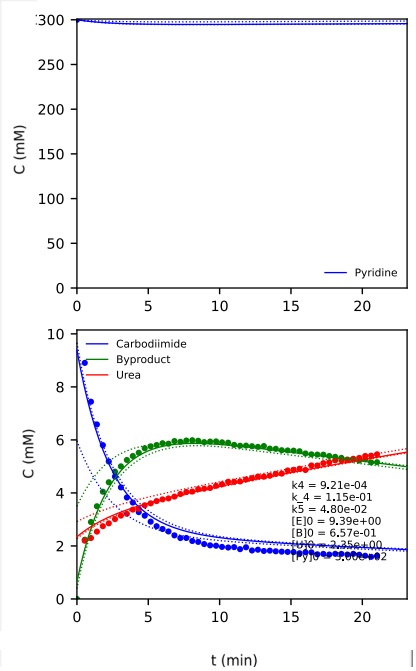

Figure S35: 300 mM MeOPy, 75 mM DMA, 12.5 mM mEDC in D_2O at pD 5.5

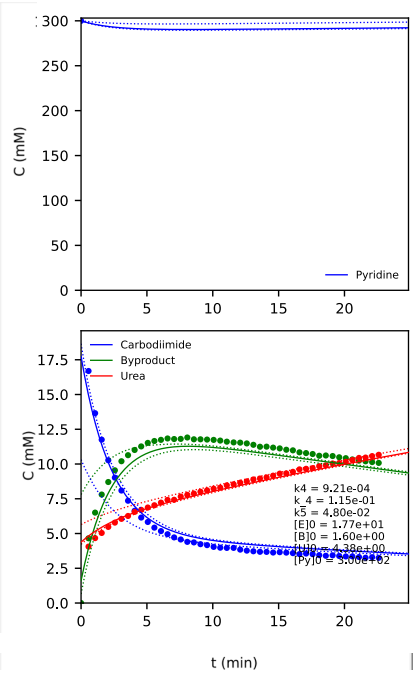

Figure S36: 300 mM MeOPy, 75 mM DMA, 25 mM mEDC in D_2O at pD 5.5

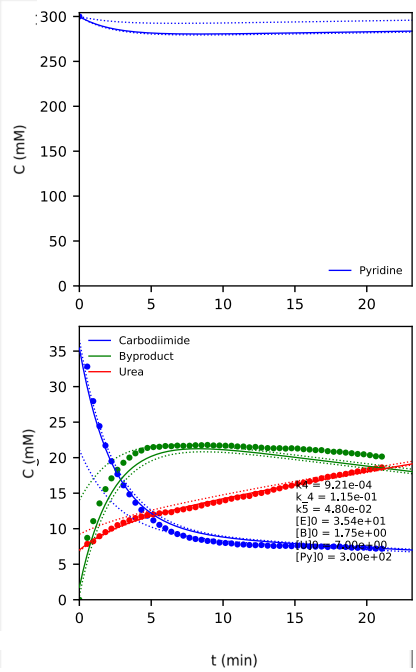

Figure S37: 300 mM MeOPy, 75 mM DMA, 50 mM mEDC in D_2O at pD 5.5

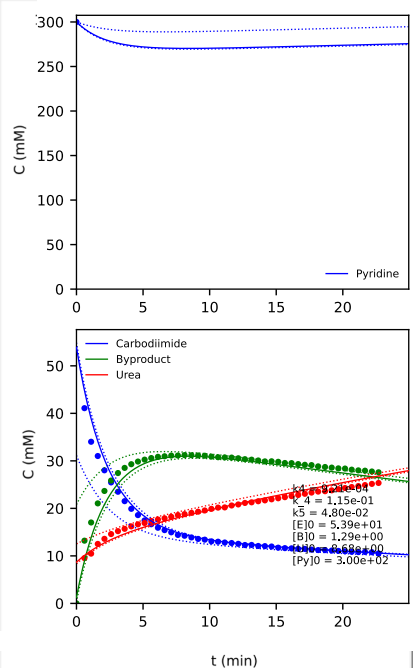

Figure S38: 300 mM MeOPy, 75 mM DMA, 75 mM mEDC in D_2O at pD 5.5

Confidence contour heat maps confirmed that the rate constants were constrained (Figure S39). For a description of a confidence contour and their utility, see the paragraph above Figure S21.

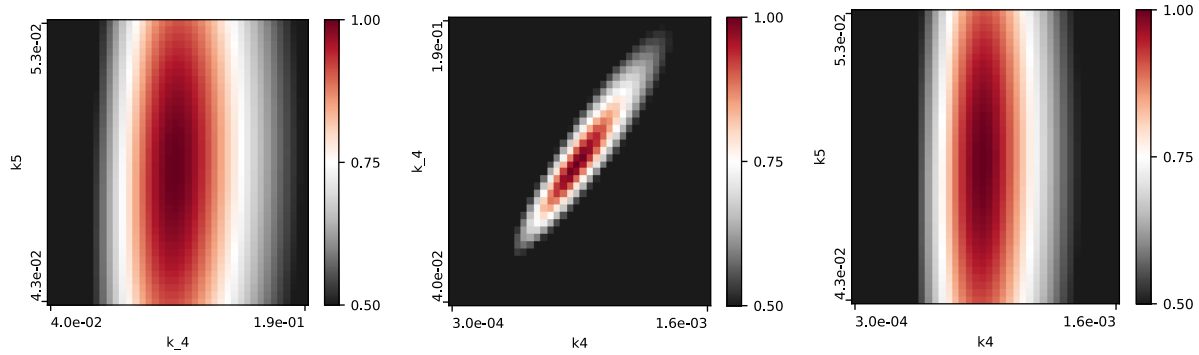

Figure S39: Confidence Contours for MeOPy Adduct Optimization System.k_4 is in units of mM^{-1} min^{-1}, k_{-4} is in units of min^{-1}, k_5 is in units of min^{-1}.

100 mM Py/MePy/MeOPy Data

We followed the change in concentration over time for both 100 and 300 mM pyridines with 75 mM mEDC. The 300 mM data is Figure 1 and the 100 mM data is available below as Figure S40.

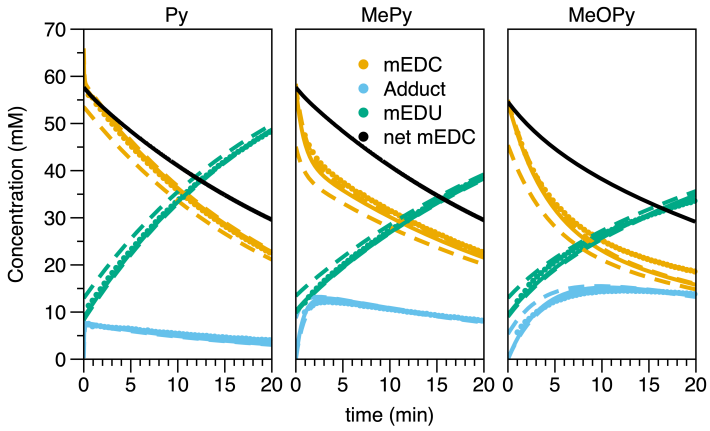

Figure S40: Change in mEDC, adduct, urea, and net mEDC (sum of mEDC and adduct) concentrations over time with 100 mM pyridines. Model fits and 95% error ranges are included.

The difference in adduct concentration between the 100 mM system (Figure S40) and the 300 mM system (Figure 1) is between two- and threefold. At about 5 minutes, the concentration of adduct in 100 mM Py is 6.4 mM, and in 300 mM Py it is 14 mM. In 100 mM MePy it is 12 mM, and in 300 mM MePy it is 28 mM. In 100 mM MeOPy it is 12 mM and in 300 mM MeOPy it is 30 mM. This corresponds to 2.2-fold increase for Py, a 2.3-fold increase for MePy, and a 2.5-fold increase for MeOPy.

Ac System

These data were not obtained from premixed samples. The mEDC and the pyridines were combined at the start of these experiments. The fits are derived from Eqs S7-27. Additional experiments were completed; however, a random number generator was used to select the experiments we used. We did this so that one set of Ac concentrations did not far outnumber the others. All experiments were completed at room temperature.

Py plots. Figures S41-50 contain the kinmodel outputs for the Py Ac system. All of the below were fit together to yield one set of rate constants.

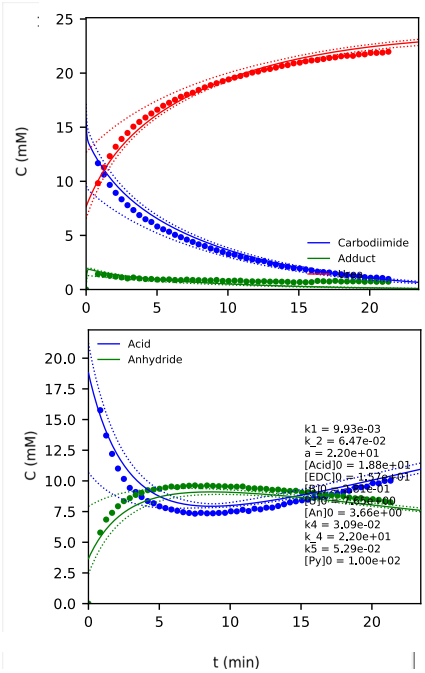

Figure S41: 100 mM Py, 25 mM Ac, 75 mM DMA, 25 mM mEDC in D_2O at pD 5.5

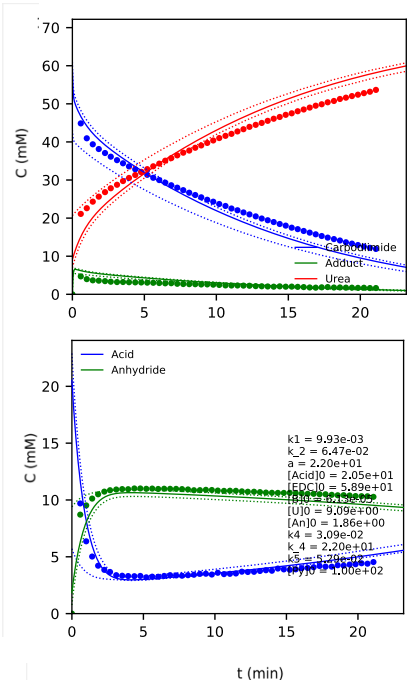

Figure S42: 100 mM Py, 25 mM Ac, 75 mM DMA, 75 mM mEDC in D_2O at pD 5.5

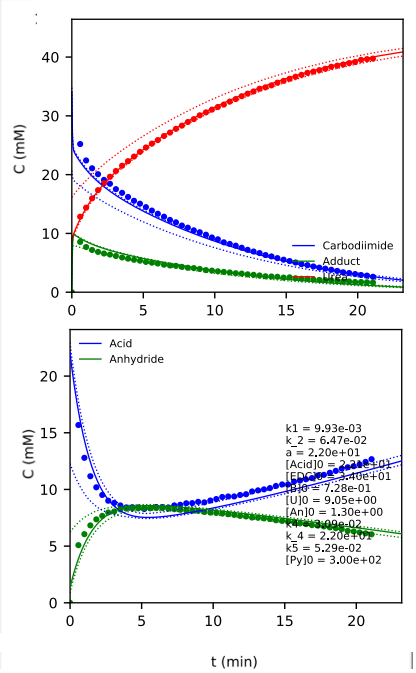

Figure S43: 300 mM Py, 25 mM Ac, 75 mM DMA, 50 mM mEDC in D_2O at pD 5.5

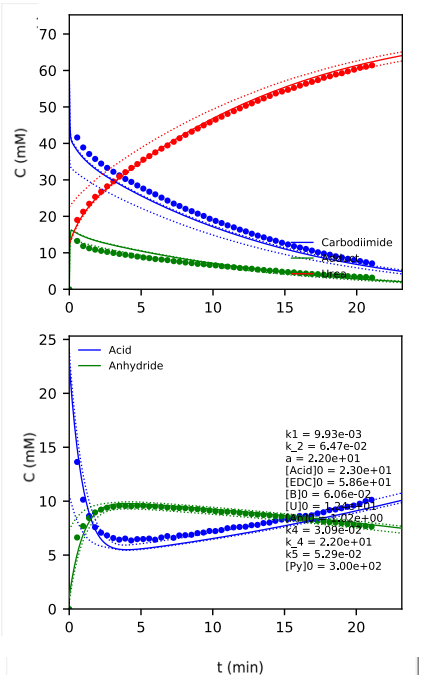

Figure S44: 300 mM Py, 25 mM Ac, 75 mM DMA, 75 mM mEDC in D_2O at pD 5.5

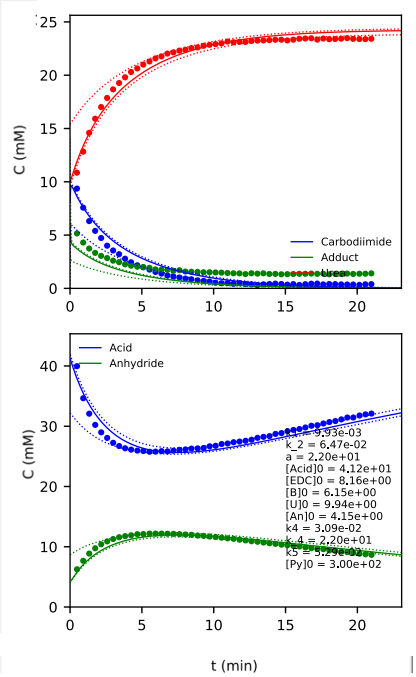

Figure S45: 300 mM Py, 50 mM Ac, 75 mM DMA, 25 mM mEDC in D_2O at pD 5.5

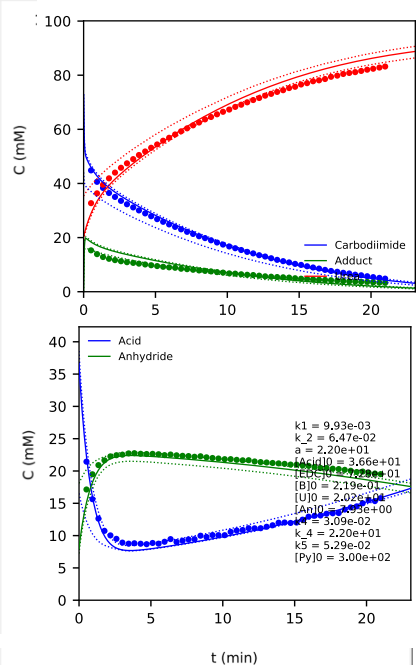

Figure S46: 300 mM Py, 50 mM Ac, 75 mM DMA, 100 mM mEDC in D_2O at pD 5.5

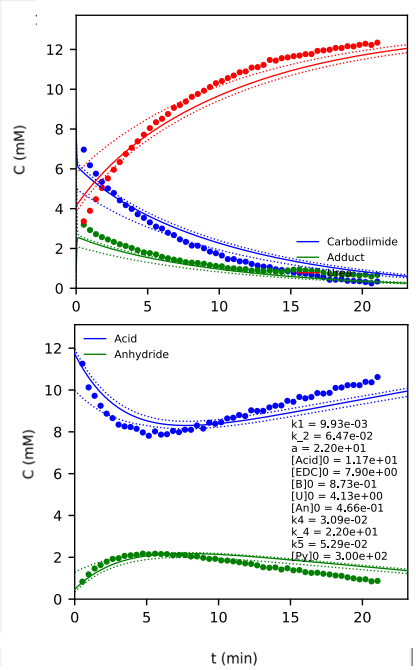

Figure S47: 300 mM Py, 12.5 mM Ac, 75 mM DMA, 12.5 mM mEDC in D_2O at pD 5.5

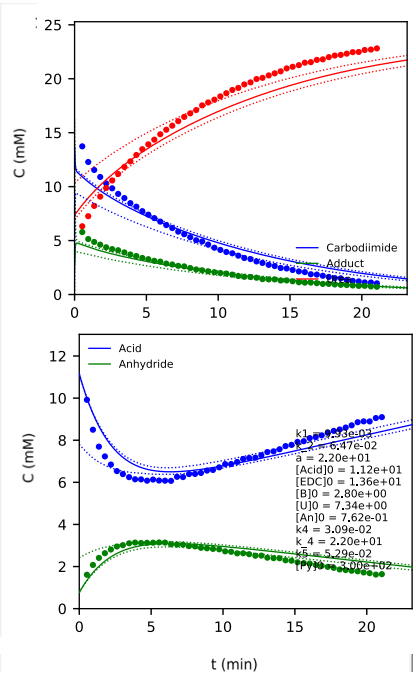

Figure S48: 300 mM Py, 12.5 mM Ac, 75 mM DMA, 25 mM mEDC in D_2O at pD 5.5

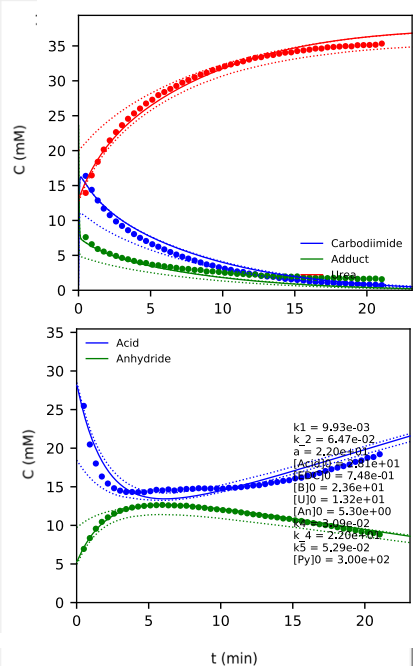

Figure S49: 300 mM Py, 37.5 mM Ac, 75 mM DMA, 37.5 mM mEDC in D_2O at pD 5.5

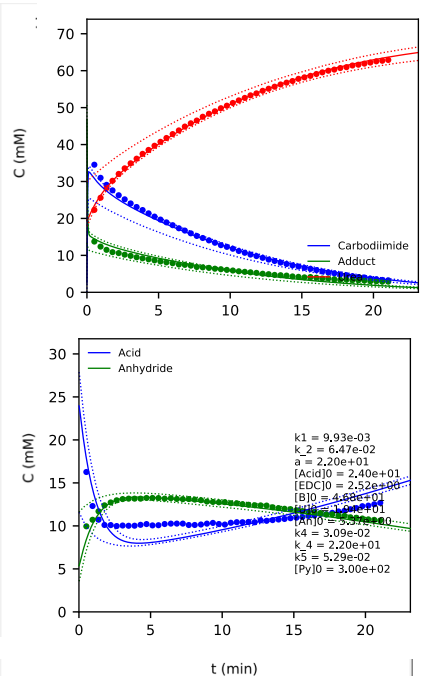

Figure S50: 300 mM Py, 37.5 mM Ac, 75 mM DMA, 75 mM mEDC in D_2O at pD 5.5

Confidence contours, here, revealed a correlation between α and k_{-2} (Figure S51). For a description of a confidence contour and their utility, see the paragraph above Figure S21.

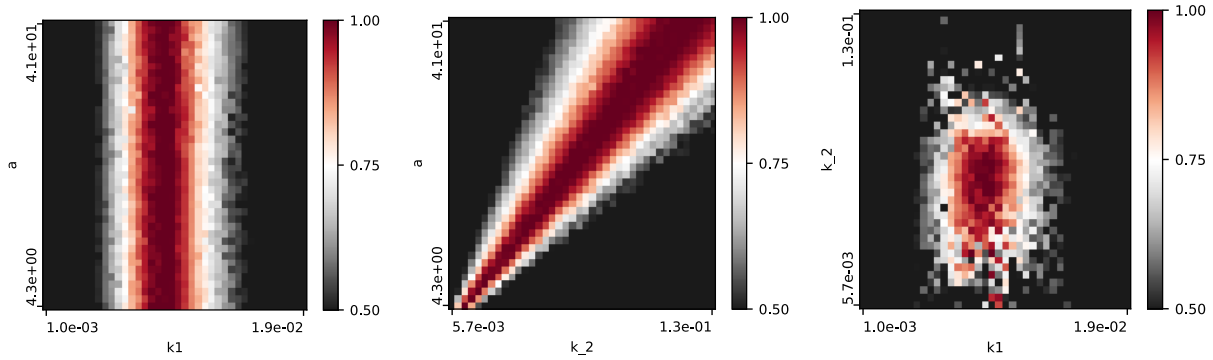

Figure S51: Confidence contours for Py with Ac (from the model with the pyridine curve on the top). Both 300 and 100 mM Py experiments were fit together to one model. k_1 is in units of mM^{-1} min^{-1}, k_{-2} is in units of mM^{-1} min^{-1}, a is in units of mM^{-1}, k_5 is in units of min^{-1}.

MePy plots. Figures S52-S62 contain the kinmodel outputs for the 4-methylpyridine (MePy) Ac system. All of the below were fit together to yield one set of rate constants.

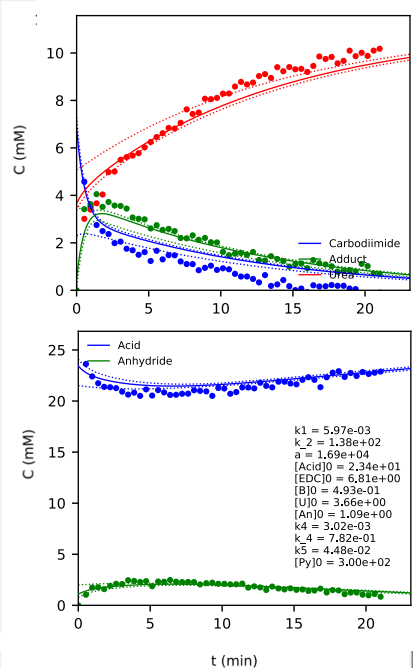

Figure S52: 100 mM MePy, 25 mM Ac, 75 mM DMA, 50 mM mEDC in D_2O at pD 5.5

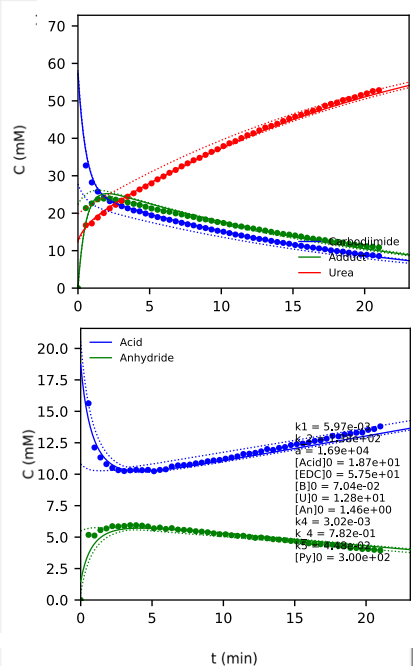

Figure S53: 100 mM MePy, 25 mM Ac, 75 mM DMA, 75 mM mEDC in D_2O at pD 5.5

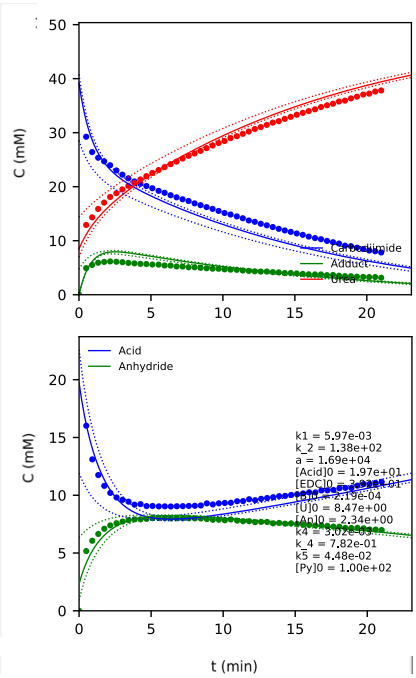

Figure S54: 300 mM MePy, 25 mM Ac, 75 mM DMA, 12.5 mM mEDC in D_2O at pD 5.5

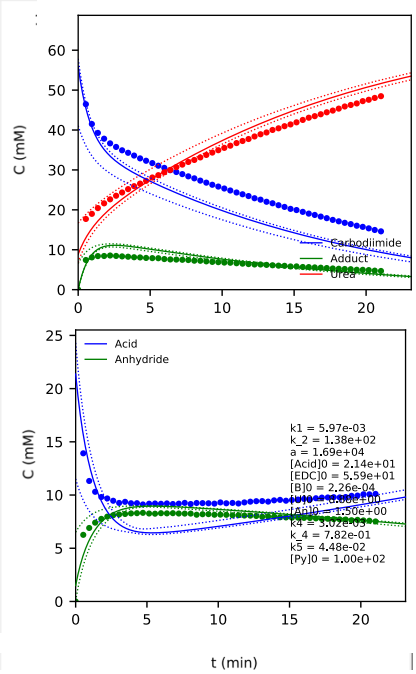

Figure S55: 300 mM MePy, 25 mM Ac, 75 mM DMA, 75 mM mEDC in D_2O at pD 5.5

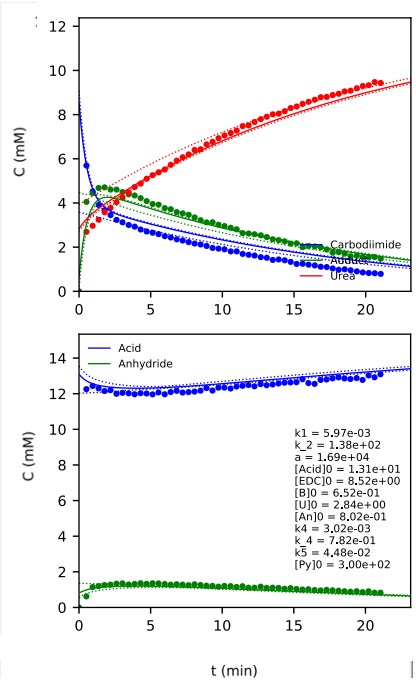

Figure S56: 300 mM MePy, 12.5 mM Ac, 75 mM DMA, 12.5 mM mEDC in D_2O at pD 5.5

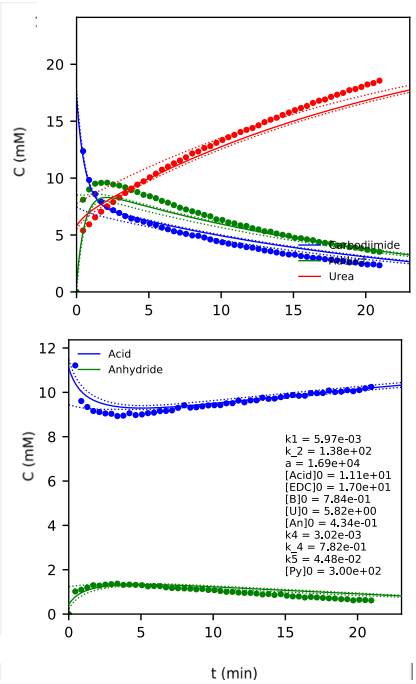

Figure S57: 300 mM MePy, 12.5 mM Ac, 75 mM DMA, 25 mM mEDC in D_2O at pD 5.5

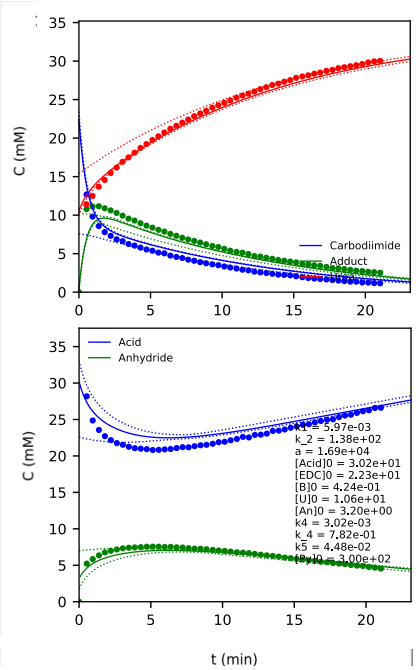

Figure S58: 300 mM MePy, 37.5 mM Ac, 75 mM DMA, 37.5 mM mEDC in D_2O at pD 5.5

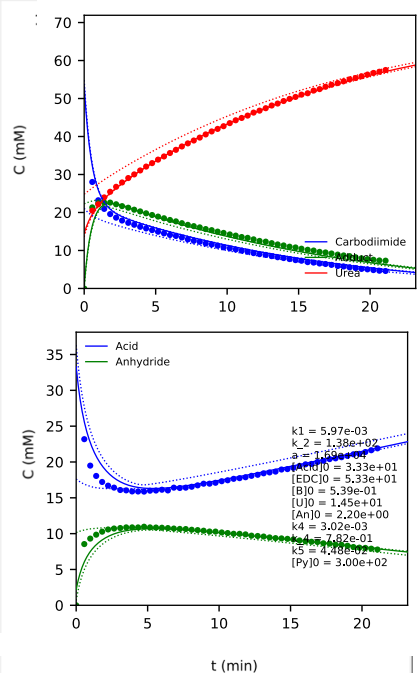

Figure S59: 300 mM MePy, 37.5 mM Ac, 75 mM DMA, 75 mM mEDC in D_2O at pD 5.5

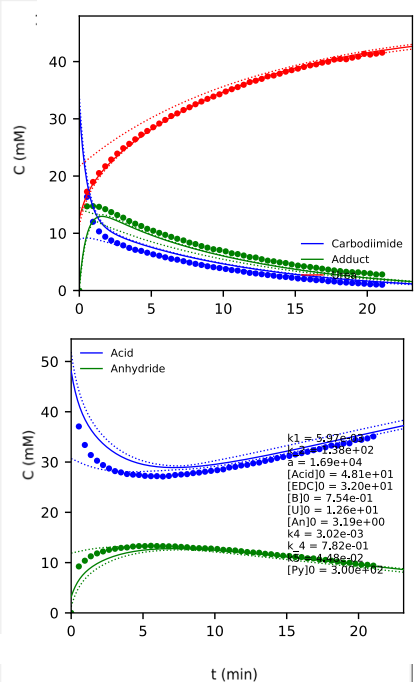

Figure S60: 300 mM MePy, 50 mM Ac, 75 mM DMA, 50 mM mEDC in D_2O at pD 5.5

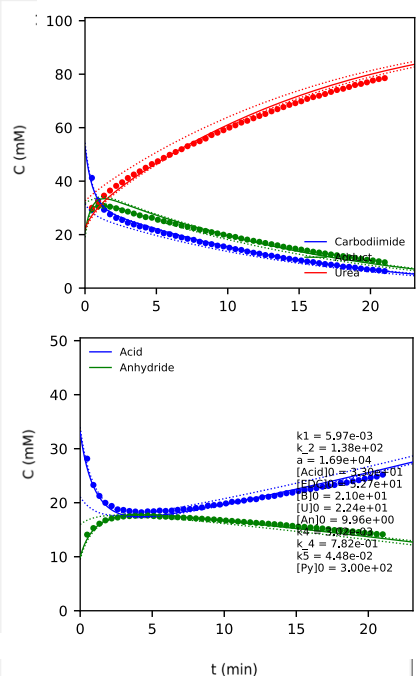

Figure S61: 300 mM MePy, 50 mM Ac, 75 mM DMA, 100 mM mEDC in D_2O at pD 5.5

Confidence contours revealed a correlation between α and k_{-2} (Figure S62). For a description of a confidence contour and their utility, see the paragraph above Figure S21.

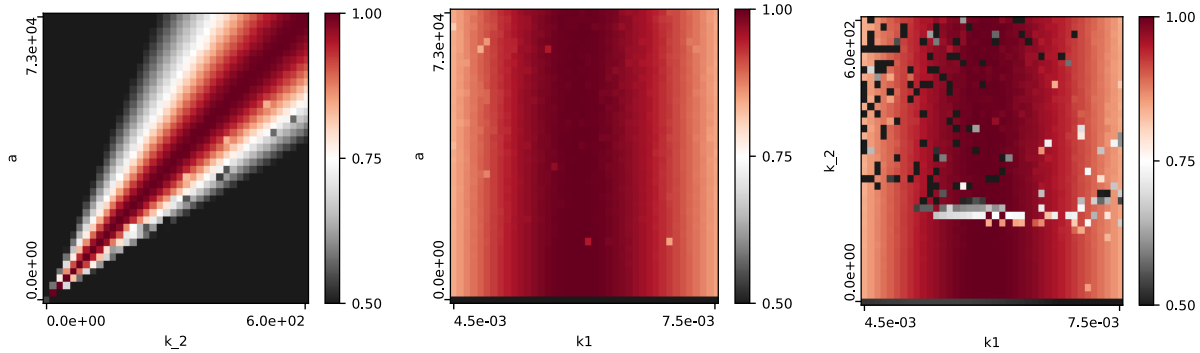

Figure S62: Confidence contours for MePy with Ac (from the model with the pyridine curve on the top). Both 300 and 100 mM MePy experiments were fit together to one model. k_1 is in units of mM^{-1} min^{-1}, k_{-2} is in units of mM^{-1} min^{-1}, a is in units of mM^{-1}, k_5 is in units of min^{-1}.

MeOPy plots. Figures S63-S73 contain the kinmodel outputs for the MeOPy Ac system. All of the below were fit together to yield one set of rate constants.

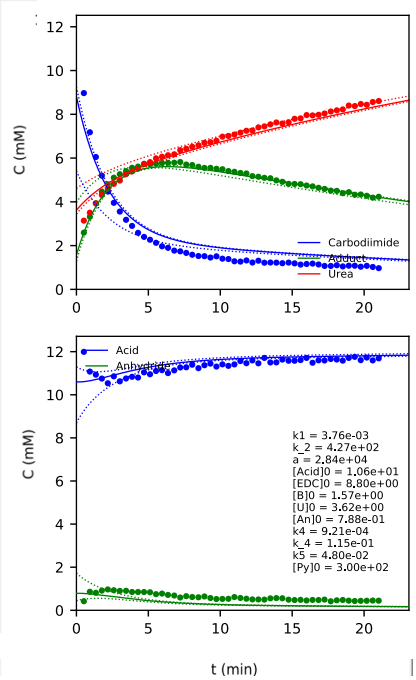

Figure S63: 300 mM MeOPy, 12.5 mM Ac, 75 mM DMA, 12.5 mM mEDC in D_2O at pD 5.5

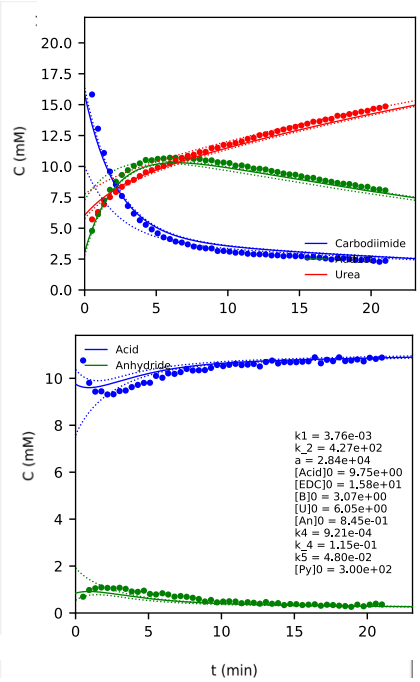

Figure S64: 300 mM MeOPy, 12.5 mM Ac, 75 mM DMA, 25 mM mEDC in D_2O at pD 5.5

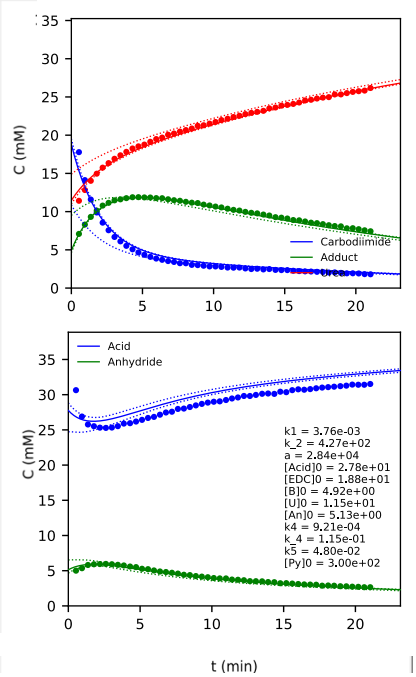

Figure S65: 300 mM MeOPy, 37.5 mM Ac, 75 mM DMA, 37.5 mM mEDC in D_2O at pD 5.5

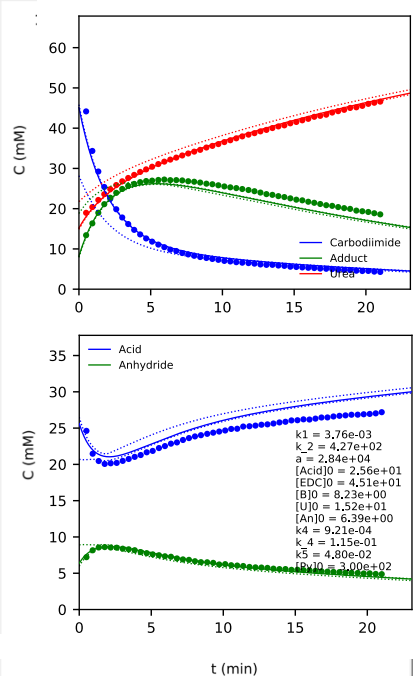

Figure S66: 300 mM MeOPy, 37.5 mM Ac, 75 mM DMA, 75 mM mEDC in D_2O at pD 5.5

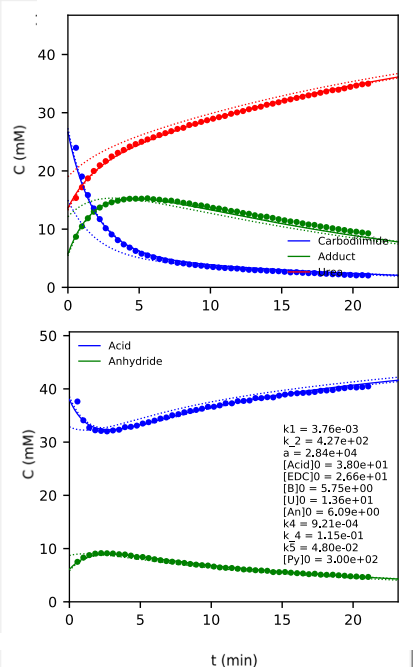

Figure S67: 300 mM MeOPy, 50 mM Ac, 75 mM DMA, 50 mM mEDC in D_2O at pD 5.5

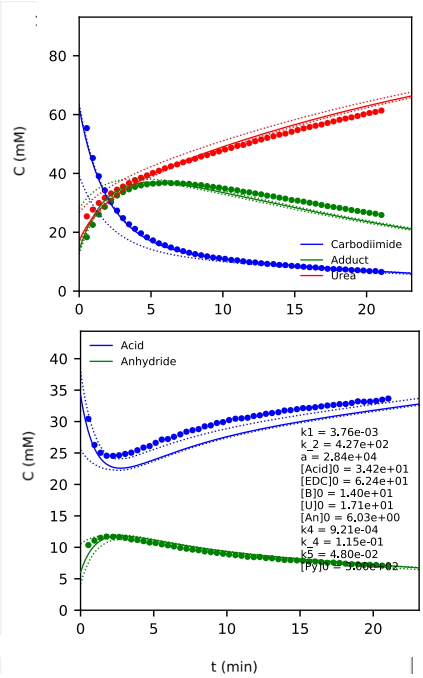

Figure S68: 300 mM MeOPy, 50 mM Ac, 75 mM DMA, 100 mM mEDC in D_2O at pD 5.5

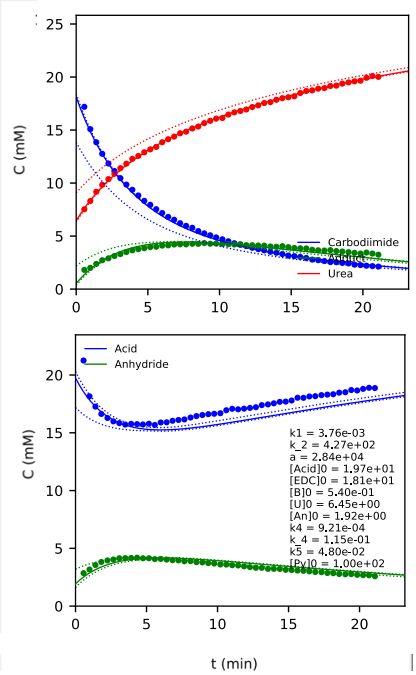

Figure S69: 100 mM MeOPy, 25 mM Ac, 75 mM DMA, 25 mM mEDC in D_2O at pD 5.5

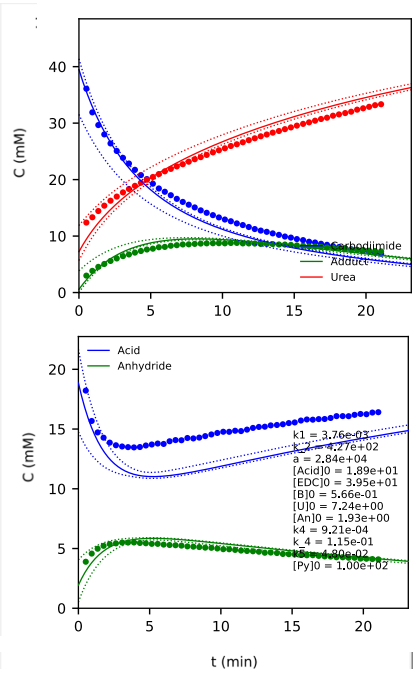

Figure S70: 100 mM MeOPy, 25 mM Ac, 75 mM DMA, 50 mM mEDC in D_2O at pD 5.5

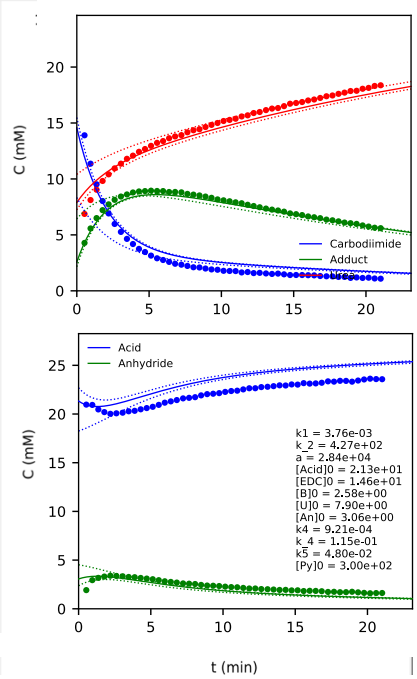

Figure S71: 300 mM MeOPy, 25 mM Ac, 75 mM DMA, 25 mM mEDC in D_2O at pD 5.5

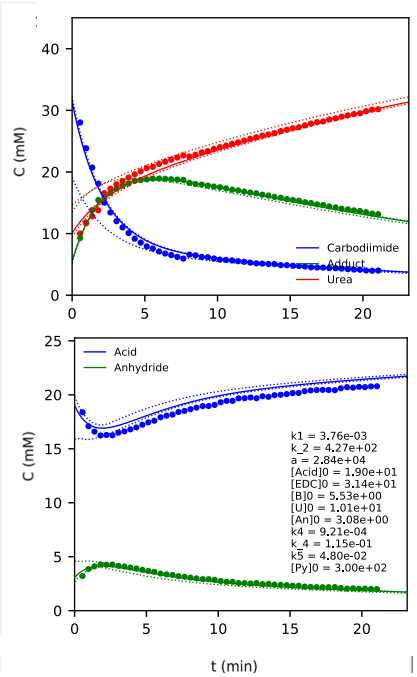

Figure S72: 300 mM MeOPy, 25 mM Ac, 75 mM DMA, 25 mM mEDC in D_2O at pD 5.5

Confidence contours revealed a correlation between α and k_{-2} (Figure S73). For a description of a confidence contour and their utility, see the paragraph above Figure S21.

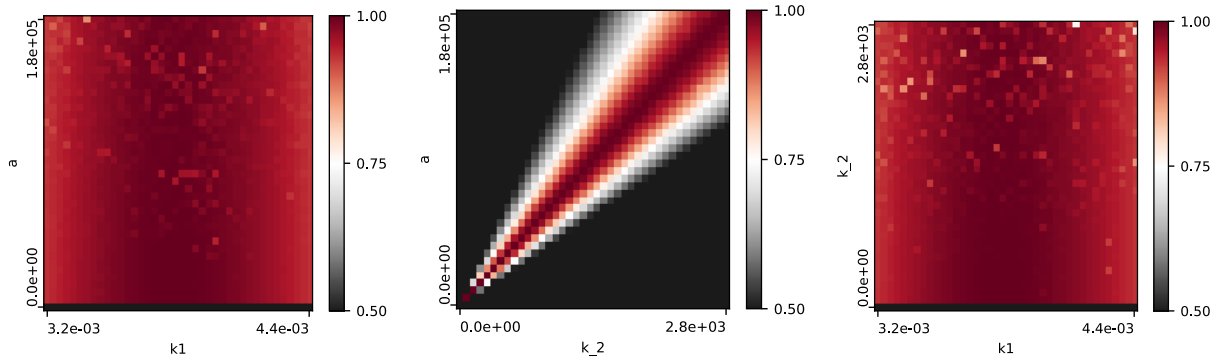

Figure S73: Confidence contours for MeOPy with Ac (from the model with the pyridine curve on the top). Both 300 and 100 mM MeOPy experiments were fit together to one model. k_1 is in units of mM^{-1} min^{-1}, k_{-2} is in units of mM^{-1} min^{-1}, a is in units of mM^{-1}, k_5 is in units of min^{-1}.

EDC Kinetic Fit

We fit an EDC system to our kinetics model in Eqs S7-S27 above, but forced k_4 and k_{-4} to be equal to zero (Figures S74-75). Rate parameters from this figure and the mEDC data are compared below in Table S1.

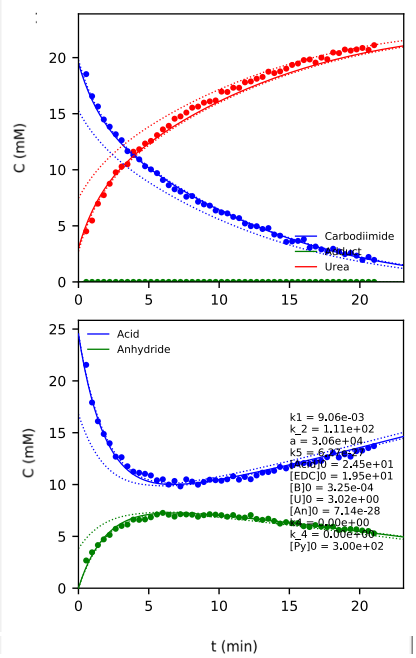

Figure S74: EDC kinetic model fits for 300 mM Py, 25 mM Ac, 25 mM EDC, 75 mM DMA in D_2O at pD 5.5.

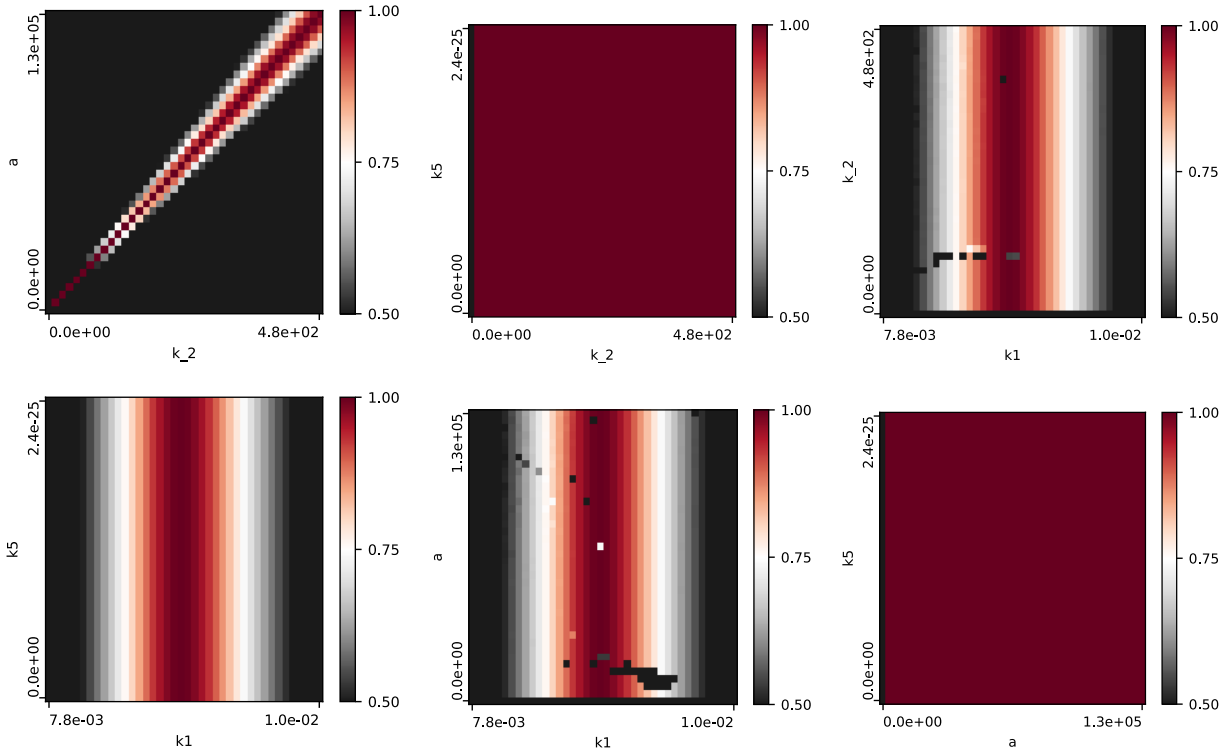

Figure S75: Confidence Contours for Figure S74. It exhibits correlated k_{-2} and a parameters with a slope of roughly 270 min. k_1 is in units of mM^{-1} min^{-1}, k_{-2} is in units of mM^{-1} min^{-1}, a is in units of mM^{-1}, k_5 is in units of min^{-1}, k_4 is in units of mM^{-1} min^{-1}, k_{-4} is in units of min^{-1}, k_5 is in units of min^{-1}.

9. Experiments not Kinetically Fitted

Premixing Comparison

In our procedure, we premixed the pyridine with the mEDC to maximize adduct concentration in the runs meant to demonstrate the effect of the adduct. This is a set of two systems of 300 mM MeOPy, 50 mM Ac, and 100 mM mEDC in D_2O at pD 5.5 with and without this 5 min premixing step. Figure S76 demonstrates the effect of this step. Note the substantially larger adduct concentration in the premixing experiment (left). The side product was not noted in the non-premixing experiment on this timescale.

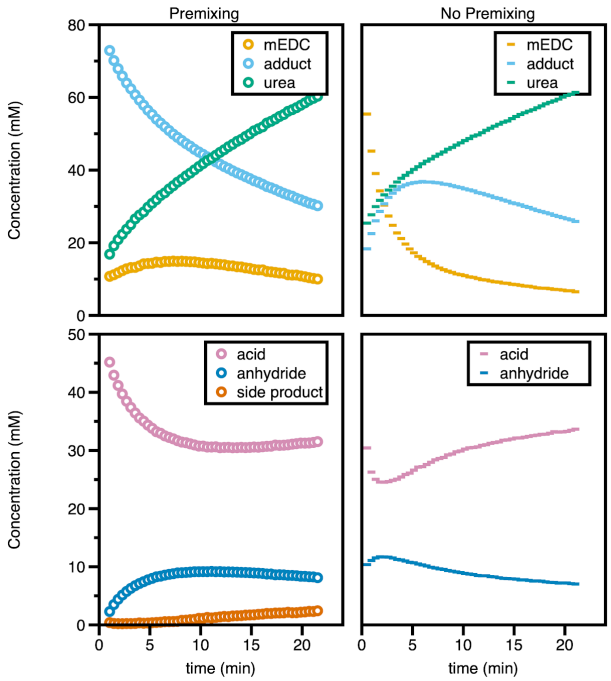

Figure S76: A comparison of the Ac system with and without the 5 min premixing step. The premixing experiment (left) was scaled from raw ^{1}H NMR integral values. See Section 2 (pages S5-6) for further information.

Anhydride Concentrations with Various Concentrations of MeOPy

We can compare the change in anhydride concentration over time for different concentrations of MeOPy. Figure S77 shows an EDC system (with no adduct) with 100, 200, and 300 mM MeOPy, which shows a decrease in lifetime of the anhydride as the MeOPy concentration increases. Here, the lifetime is defined as the time for the Ac to return to 60% of its maximum concentration (since the 100 mM system never returns to the 80% parameter used elsewhere, due to side product formation and experiment length). It has 52 min for 100 mM, 36 min for 200 mM, and 24 min for 300 mM. For the EDC system, there is no decrease in maximum anhydride concentration (100 mM: 12 mM at 7 min, 200 mM: 13 mM at 4 min, 300 mM: 12 mM at 6 min).

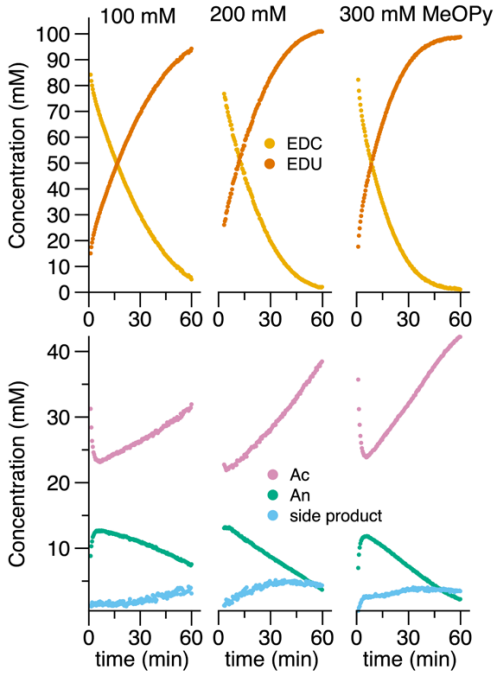

Figure S77: 100 mM, 200 mM, and 300 mM MeOPy, respectively, with 50 mM Ac, 75 mM DMA, 100 mM EDC in D_2O at pD 5.5. These experiments were scaled from raw ^1H NMR integral values. See Section 2 (pages S5-6) for further information.

Figure S78 shows an mEDC system (with adduct) at 100, 300, and 600 mM MeOPy, which shows a decrease in the maximum An concentration (100 mM: 12 mM at 11 min, 300 mM: 9 mM at 12 min, 600 mM: 6 mM at 9 min), though, qualitatively, less of a decrease in An lifetimes. Exact lifetimes are not obtainable using previous methods due to the abundance of the side product in these experiments.

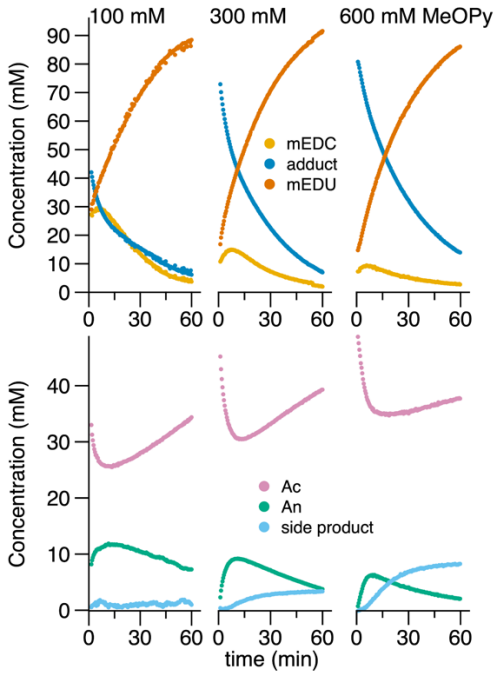

Figure S78: 100 mM, 300 mM, and 600 mM MeOPy, respectively, with 50 mM Ac, 75 mM DMA, 100 mM mEDC in D_2O at pD 5.5. These experiments were scaled from raw ^1H NMR integral values. See Section 2 (pages S5-6) for further information.

Interestingly, Figures S77 and S78 show different behavior in the presence and absence of adduct. Increased MeOPy concentration leads to an decreased An lifetime in the EDC system, though no change in the maximum An concentration. In the mEDC system, the maximum An concentration changes much more, but the lifetime is much less affected (qualitatively).

EDC vs mEDC KSBA Anhydride Formation

We replicated the results for Ac with 4-sulfobenzoic acid monopotassium salt (KSBA) (Figure S79).

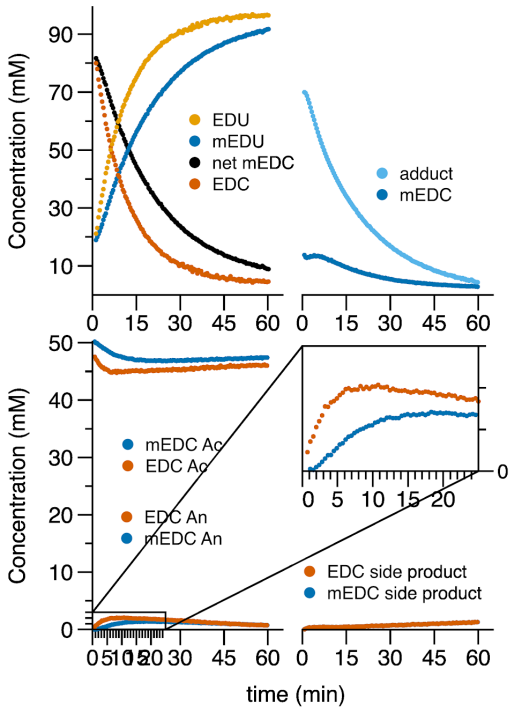

Figure S79: Changes in concentrations over time for 100 mM mEDC vs EDC in 300 mM MeOPy and 50 mM 4-Sulfobenzoic acid monopotassium salt (KSBA) with a 75 mM N,N-dimethylacetamide internal standard in D_2O at pD 5.5 and room temperature. These experiments were scaled from raw ^1H NMR integral values. See Section 2 (pages S5-6) for further information.

This experiment demonstrated that the time to maximum anhydride concentration was extended for mEDC vs EDC (1.4 mM at 18 min vs 2.1 mM at 11 min) and the net mEDC concentration was increased when compared to EDC, though the anhydride yield was dramatically lower than for Ac. The anhydride concentrations are too low for a meaningful comparison of their lifetimes.

Full Timescale for mEDC Ac System

In the main text, we omitted the entire timescale of the 300 mM MeOPy system for the sake of comparison. The entire experiment is visible below as Figure S80.

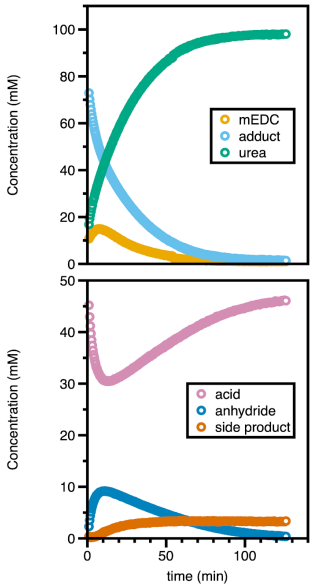

Figure S80: Full timescale for 300 mM MeOPy mEDC experiment, see Figure 2. This experiment was scaled from raw ^{1}H NMR integral values. See Section 2 (pages S5-6) for further information.

Comparison of Anhydride Concentrations with Py/MePy/MeOPy

We can compare the change in anhydride concentration over time for Py, MePy, and MeOPy. As Figure S81 shows, the concentration of anhydride is reduced from Py to MePy to MeOPy.

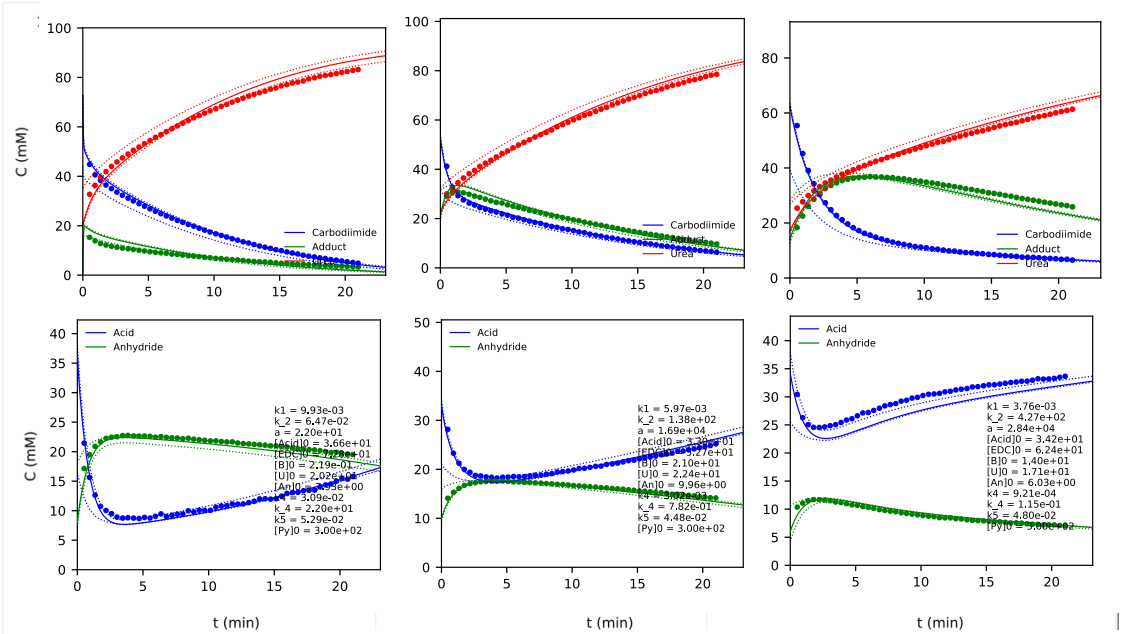

Figure S81: 300 mM Py, MePy, and MeOPy, respectively, with 50 mM Ac, 75 mM DMA, 100 mM mEDC in D_2O at pD 5.5.

Figure S82 shows that the concentration of anhydride and its lifetime is similarly reduced from Py to MePy to MeOPy. The maximum anhydride concentration is 25.8 mM for Py, 16.1 mM for MePy, and 11.9 mM for MeOPy.

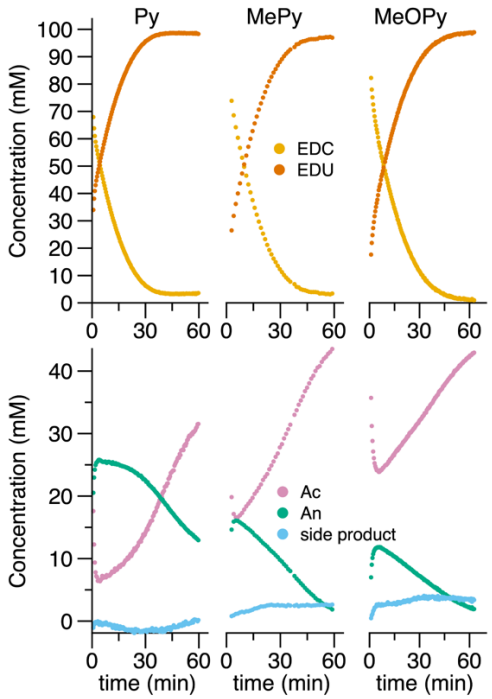

Figure S82: 300 mM Py, MePy, and MeOPy, respectively, with 50 mM Ac, 75 mM DMA, 100 mM EDC in D_2O at pD 5.5. These experiments were scaled from raw ^1H NMR integral values. See Section 2 (pages S5-6) for further information.

2-Methylpyridine Buffer Data

To test the degree to which the formation of the adduct can tolerate pyridine functionality in positions other than the *para* position, we completed an experiment with 2-methylpyridine as the buffer (Figure S83).

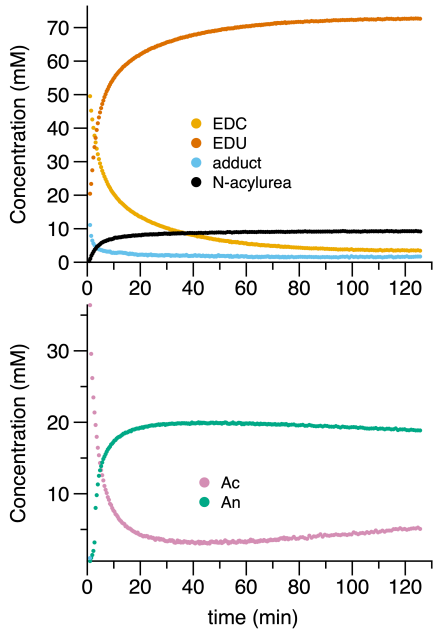

Figure S83: Concentration changes over time for 300 mM 2-methylpyridine, 100 mM mEDC, 50 mM Ac, and 75 mM *N,N*-dimethylacetamide in D_2O at pD 5.5. The adduct was pre-concentrated by premixing it for 2 min 35 s.

We observed a much slower hydrolysis of the anhydride, very little adduct formation, and negligible formation of the side product, along with a substantial amount of N-acylurea generated. We hypothesize that the sterically hindered pyridine cannot easily form the acylpyridinium, which is essential for the formation of the side product and the decomposition of the anhydride. It also is hindered from attacking the carbodiimide to form the adduct. In addition, it fails to remove the N-acylurea byproduct.

10. Side Product Observations and Proposed Structure

A side product was observed that does not fit with Eqs 3-8. It is transient but long-lived, as Figure S84 demonstrates.

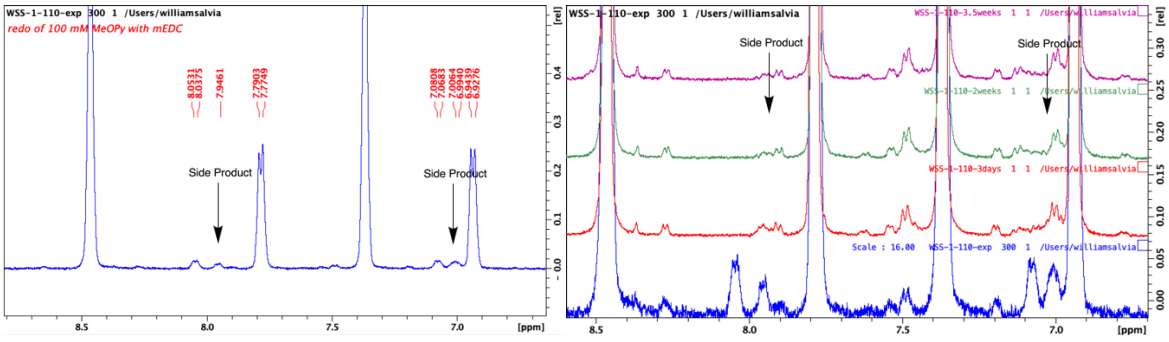

Figure S84: NMR spectra showing peak assignments at the end of the experiment after roughly 2 hours (left). An is observed as a doublet around 8.04 ppm and 7.07 ppm, the side product is visible at around 7.00 and 7.95 ppm, and Ac is visible at around 6.93 and 7.78 ppm. After three days, 2 weeks, and three and a half weeks, new spectra (red, green, and magenta, respectively) were taken

and compared with the 2 h scan (blue) on the right. The 2 h spectrum was scaled up by a factor of 16 since it is only a single ^{1}H NMR scan, compared to the 3.5-week spectrum's 16 combined scans. The side product is nearly gone by 3 days and is minimal in later spectra.

The species is present at ~7.00 ppm and ~7.95 ppm in the spectrum taken after 2 h and is not significantly present by 3.5 weeks. The side product in the 2 h spectrum is estimated by relative integral values to be roughly 4% of the total of the acid, anhydride, and side product signals. In the 3.5 week spectrum, it is less than 1% of the total, though an exact value is impacted by noise.

We then investigated the conditions under which this side product forms and identified that it also forms in the absence of mEDC, when 25 mM An is combined with a 300 mM MeOPy solution buffered in D_2O at pD 5.5 (Figure S85).

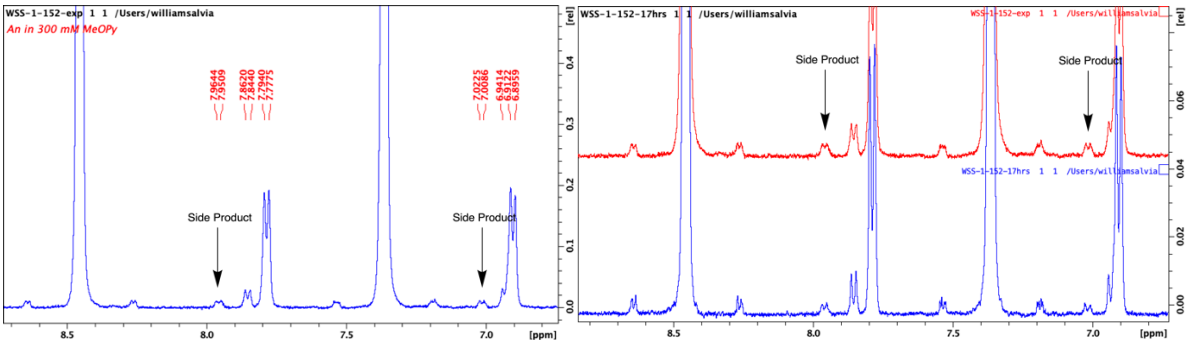

Figure S85: 25 mM An in 300 mM MeOPy at pD 5.5. Two spectra were taken, one (left, top right) was taken about a minute after the An and MeOPy solutions were combined. The other (bottom right) was taken at 17 h. No An peak was detected. The side product is present at ~7.95 and ~7.00 ppm, Ac is present at ~7.78 and ~6.90 ppm, and an additional side product that does not form in our normal system is present at ~7.85 and ~6.94 ppm. The chemical shifts were calibrated using MeOPy's rightmost peak, since there was no internal standard present.

The side product is also transient in this An system. Based on integral values, the side product makes up about 5.3% of the total acid/anhydride/side product species at 1 min, and about 3.7% at 17 h.

Figure S85 demonstrates that the side product was observed when the only species present at the start of the experiment are MeOPy and An. From other experiments we know that the side product forms when 4-sulfobenzoic acid monopotassium salt (KSBA) is used instead of Ac (Figure S79), as well as with Py, MePy, and MeOPy (Figure S82). This means that neither a specific carboxylic acid nor specific pyridine derivative is necessary to form this side product. However, the pyridine is probably involved, since increased concentration of MeOPy leads to a higher concentration of side product (Figure S78). Since it is transient (Figure S84), it must exist at equilibrium with the other species in the system. It also does not form when 2-methylpyridine is used, which does not form the acylpyridinium easily (Figure S83). We propose that it is derived from the reaction of water and the known acylpyridinium intermediate (Scheme S3).

Scheme S3: The mechanism of formation and structure of our proposed side product identification (avg. n = 11 - 12).

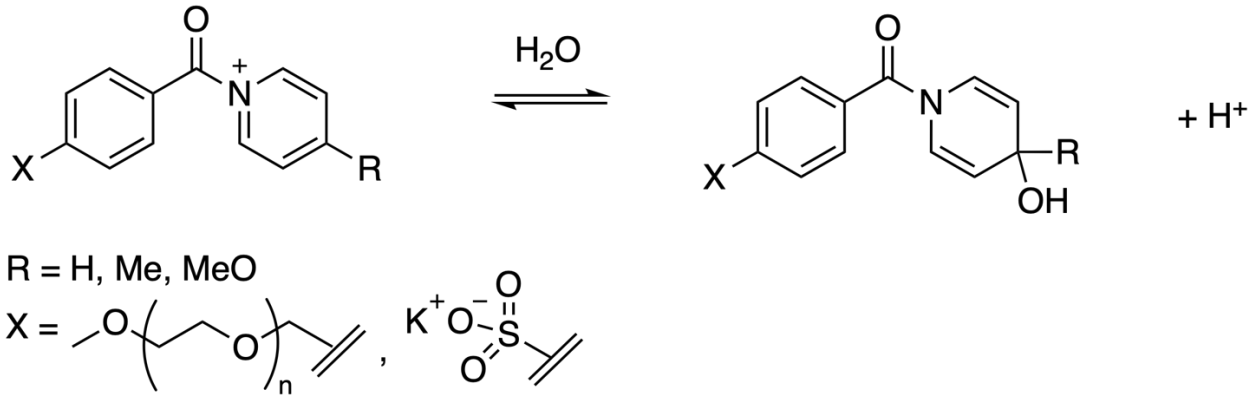

11. Fit Parameters

The rate constants for this paper were derived using kinetics software "kinmodel", found within the Supporting Information of the published work: *J. Org. Chem.* **2020**, *85*, 682–690[2].

EDC/mEDC

We compared rate parameters for EDC and mEDC under our reaction conditions (Figures S41-50 and S74). Descriptions of these rate parameters can be found in Eqs 3-8. Both mEDC and EDC exhibit correlated k_{-2} and a parameter with a similar ratio of ~300 (Figures S51, S84). As expected, mEDC demonstrates an increased direct hydrolysis rate (k_5). However, mEDC and EDC, surprisingly, have similar reactivity towards Ac under our conditions (Table S1). Within confidence intervals EDC and mEDC's k_1's are equal, despite the carbodiimides' distinct structures and properties.

Table S1: Rate parameters for the reaction of mEDC and EDC in Py.

Carbodiimide	k_1 (M^{-1} min^{-1})	k_{-2} (M^{-1} min^{-1})	a (M^{-1})	k_5 (min^{-1})
mEDC	9.93×10^{-3} (8.99×10^{-3} to 1.02×10^{-2})	6.47×10^{-2} (5.85×10^{-2} to 6.86×10^{-2})	2.20×10^{1} (2.10×10^{1} to 2.40×10^{1})	5.29×10^{-2} (5.27×10^{-2} to 5.32×10^{-2})
EDC	9.06×10^{-3} (8.84×10^{-3} to 9.30×10^{-3})	1.11×10^{2} (6.68×10^{1} to 1.68×10^{2})	3.06×10^{4} (1.84×10^{4} to 4.61×10^{4})	~0*

* 6.27×10^{-27} (4.70×10^{-29} to 1.55×10^{-7}) min^{-1} was the exact result, but, based on confidence contours in Figure S84, the rate of hydrolysis was so slow that the model could not determine it.

Py/MePy/MeOPy

Table S2 contains the rate constants for Eqs 1-2. Py had a correlation between k_4 and k_{-4} that resulted from the fast addition of the pyridine to the carbodiimide. The errors ranges are a 95% confidence range acquired by bootstrapping using the random-X method (10000 permutations).

Table S2: Rate constant data for Py, MePy and MeOPy, following Eqs 1-2.

	Py	MePy	MeOPy
k_4 (M^{-1} min^{-1})	n/a	3.0 (2.4 to 3.6)	9.2×10^{-1} (7.9×10^{-1} to 9.7×10^{-1})
k_{-4} (min^{-1})	n/a	7.8×10^{-1} (6.3×10^{-1} to 9.6×10^{-1})	1.1×10^{-1} (9.9×10^{-2} to 1.2×10^{-1})
K (k_4/k_{-4}) (M^{-1})	1.4	3.9	8.4
k_5 (min^{-1})	5.29×10^{-2} (5.27×10^{-2} to 5.32×10^{-2})	4.48×10^{-2} (4.44×10^{-2} to 4.55×10^{-2})	4.80×10^{-2} (4.71×10^{-2} to 4.87×10^{-2})

Based on this data, we produced the Hammett plot for K in Figure S86.[5]

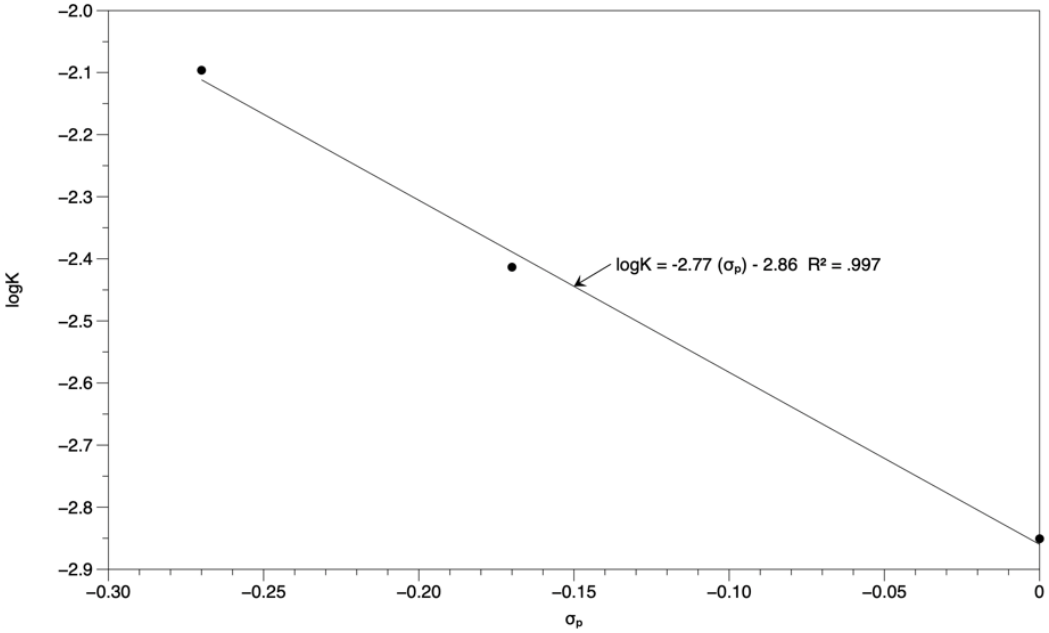

Figure S86: A Hammett Plot for $K = k_4/k_{-4}$ for the Ac model (Eq 3-8).

This plot has a negative slope with a significant p-value of 3.6%, calculated in Excel via ANOVA (Table S3).

Table S3: Standard Error and p-value for *K* Hammett Plot

	Coefficients	Standard Error	p-value
Intercept	-2.86	0.029	.0065
Slope	-2.77	0.16	.036

We also completed carbodiimide-driven Ac experiments with Py and MePy at both 100 and 300 mM, as well as MeOPy at 100 mM, in addition to the results available in the main text for 300 mM MeOPy. These results can be seen in the above section of this SI.

For the Ac system, work by Ferscht and Jencks (1970) was used to find the trend of k_{-2}. This is based on their work on the hydrolysis of acetate by Py, MePy, and MeOPy (Table S4).[6] We can roughly estimate values for the rate constant α based on the correlated contour plots contained in

Figures S51, S62, and S73, above. The estimated values of α should be considered primarily for comparison, relative to one another. They should not be taken as neither accurate nor substantially variable values of α; we considered them roughly equivalent.

Table S4: Trend of k_{-2} for Py, MePy, and MeOPy, along with a rough estimate of α for each for the purposes of comparison.

Pyridine	k_{-2} for acetic anhydride[6] (M^{-1} min^{-1})	Line of Best Fit for k_{-2} vs α confidence contour (slope units: min)	Estimated α value given k_{-2} estimate (M^{-1})
Py	5.0×10^{3}	$\alpha = 300 \times k_{-2}$	2×10^{6}
MePy	2.9×10^{4}	$\alpha = 120 \times k_{-2}$	3×10^{6}
MeOPy	5.6×10^{4}	$\alpha = 64 \times k_{-2}$	4×10^{6}

12. References

(1) Glasoe, P. K.; Long, F. A. Use of Glass Electrodes to Measure Acidities in Deuterium Oxide. *J. Phys. Chem.* **1960**, *64* (1), 188–190. https://doi.org/10.1021/j100830a521.

(2) Kariyawasam, L. S.; Kron, J. C.; Jiang, R.; Sommer, A. J.; Hartley, C. S. Structure–Property Effects in the Generation of Transient Aqueous Benzoic Acid Anhydrides by Carbodiimide Fuels. *J. Org. Chem.* **2020**, *85* (2), 682–690. https://doi.org/10.1021/acs.joc.9b02746.

(3) Krężel, A.; Bal, W. A Formula for Correlating pKa Values Determined in D2O and H2O. *J. Inorg. Biochem.* **2004**, *98* (1), 161–166. https://doi.org/10.1016/j.jinorgbio.2003.10.001.

(4) *CRC Handbook of Chemistry and Physics*, 95th ed.; Haynes, W. M., Ed.; CRC Press: Boca Raton, 2014. https://doi.org/10.1201/b17118.

(5) Hansch, Corwin.; Leo, A.; Taft, R. W. A Survey of Hammett Substituent Constants and Resonance and Field Parameters. *Chem. Rev.* **1991**, *91* (2), 165–195. https://doi.org/10.1021/cr00002a004.

(6) Fersht, A. R.; Jencks, W. P. Acetylpyridinium Ion Intermediate in Pyridine-Catalyzed Hydrolysis and Acyl Transfer Reactions of Acetic Anhydride. Observation, Kinetics, Structure-Reactivity Correlations, and Effects of Concentrated Salt Solutions. *J. Am. Chem. Soc.* **1970**, *92* (18), 5432–5442. https://doi.org/10.1021/ja00721a023.